



Cite this: *Mater. Adv.*, 2025, 6, 8740

## Advances in nitrogen-doped carbon dots for electrochemical energy storage: from synthesis to applications

Sewara J. Mohammed, <sup>\*a</sup> Awat S. Mohammed, <sup>a</sup> Kazo K. Abdalla, <sup>a</sup> Darya Sh. Hamad, <sup>b</sup> Fryad S. Mustafa, <sup>a</sup> Dana A. Kader, <sup>c</sup> Kawan F. Kayani, <sup>a</sup> Kovan K. Abdalla, <sup>d</sup> Harez R. Ahmed <sup>a</sup> and Shujahadeen B. Aziz <sup>e</sup>

Nitrogen-doped carbon dots (N-CDs) have emerged as a transformative class of carbon-based nanomaterials for next-generation electrochemical energy storage systems, owing to their outstanding electrical conductivity, tunable surface functionalities, and superior chemical stability. This review systematically explores recent advances in the synthesis of N-CDs, structural engineering strategies, and advanced characterization techniques, with an emphasis on structure–property relationships. Applications in lithium/sodium/potassium-ion batteries, supercapacitors, and metal–air batteries are critically assessed, with a focus on how nitrogen doping enhances charge transport, cycling stability, and energy density. The synergistic integration of N-CDs with metal oxides, conductive polymers, and hybrid nanostructures is also discussed as a pathway to overcome limitations of conventional electrode materials. Key challenges, including scalability, long-term cycling performance, and commercial viability, are analyzed. Finally, we highlight future research directions, including AI-guided material discovery, multifunctional composites, and eco-friendly synthesis approaches, providing a strategic roadmap for developing sustainable, high-performance energy storage technologies through the rational design of N-CD-based materials.

Received 18th August 2025,  
Accepted 20th October 2025

DOI: 10.1039/d5ma00927h

rsc.li/materials-advances

## 1 Introduction

The rapid adoption of electric vehicles, grid-connected renewable energy systems, and high-drain consumer electronics is creating a growing demand for high-performance and sustainable energy storage technologies.<sup>1–3</sup> Despite their market dominance, lithium-ion batteries (LIBs) still struggle with limited rate capability, moderate specific energy, and progressive capacity fade during long-term cycling. Similarly, supercapacitors offer exceptional power density yet are constrained by low specific energy, limiting their practical usefulness. These shortcomings have prompted intense research into advanced nanomaterials that combine high

electrical conductivity, abundant active sites, and structural stability, enabling fast, long-lasting energy storage.<sup>4–7</sup>

Carbon-based materials, particularly nanomaterials such as graphene quantum dots (GQDs), carbon nanodots (CNDs), and carbonized polymer dots (CPDs), are widely recognized as foundational components for advanced energy storage systems<sup>8</sup> and have been extensively studied for applications in sensing, photocatalysis, and bioimaging.<sup>9,10</sup> The general promise and tunable properties of quantum dots for energy storage have been comprehensively reviewed elsewhere.<sup>11</sup> Among these, carbon dots (CDs) are quasi-spherical carbon nanomaterials with sizes below 10 nm, exhibiting intriguing optical and electronic properties that are size-tunable, along with a large surface area that enables easy functionalization.<sup>7,11</sup> Nevertheless, their application in energy storage has only recently gained significant momentum, driven largely by the development of heteroatom doping techniques that dramatically enhance their electrochemical performance.<sup>12–14</sup>

Nitrogen-doped carbon dots (N-CDs) provide a real breakthrough in this prospect. Introducing nitrogen atoms into the  $sp^2$  carbon framework (Fig. 1) creates graphitic-N that donates electrons to the  $\pi$ -network, pyridinic-N that provides coordination sites, and pyrrolic-N that supports reversible redox

<sup>a</sup> Department of Chemistry, College of Science, University of Sulaimani, Qlyasan Street, Sulaymaniyah 46001, Kurdistan Regional Government, Iraq.  
E-mail: sewara.mohammed@univsul.edu.iq

<sup>b</sup> Department of Medical Microbiology, College of Health Sciences, Cihan University Sulaimaniya, Sulaymaniyah City, Kurdistan, Iraq

<sup>c</sup> Department of Chemistry, College of Education, University of Sulaimani, Old Campus, 46001, Sulaymaniyah 46001, Kurdistan Regional Government, Iraq

<sup>d</sup> State Key Laboratory of Chemical Resource Engineering, Beijing University of Chemical Technology, Beijing, China

<sup>e</sup> Research and Development Center, University of Sulaimani, Qlyasan Street, Sulaymaniyah 46001, Kurdistan Regional Government, Iraq



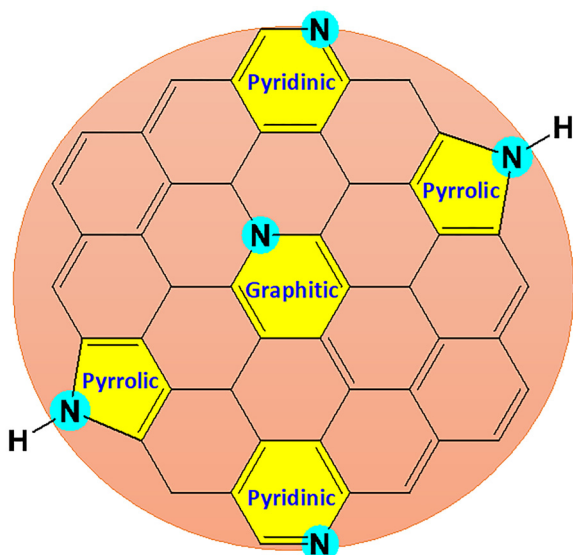


Fig. 1 Different nitrogen configurations are present in the chemical structure of N-CDs.

chemistry.<sup>15,16</sup> Collectively, these configurations improve electron transport, ion adsorption, and pseudocapacitance, positioning N-CDs as candidates for LIBs, sodium-ion batteries (SIBs), potassium-ion batteries (PIBs), metal–air batteries, and hybrid supercapacitors.<sup>4,17–19</sup>

As shown in Fig. 2, a literature search on ScienceDirect using the terms “nitrogen-doped carbon dots” in combination with “sodium-ion batteries, lithium-ion batteries, potassium-ion batteries, supercapacitors, metal–air batteries, and hybrid energy storage systems” reveals a strong growth in publications from 2010 to 2025. This trend reflects the expanding research interest in N-CDs and their potential as scalable, high-performance materials for electrochemical energy storage. Data were retrieved in July 2025.

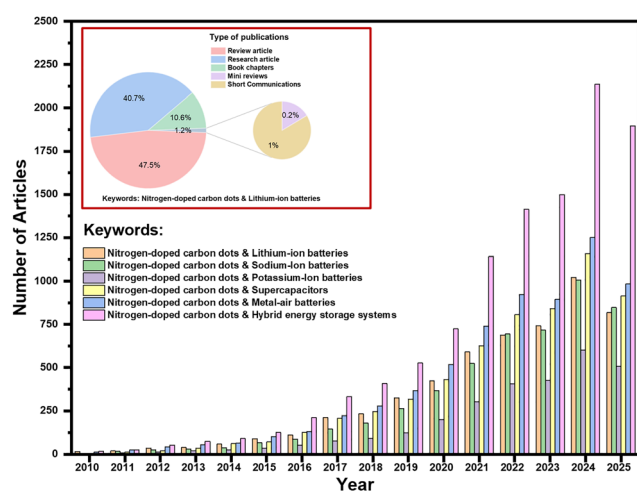


Fig. 2 Papers published on the topics of “nitrogen-doped carbon dots” and “lithium-, sodium-, and potassium-ion batteries”, as well as supercapacitors, metal–air batteries, and hybrid energy storage systems, from 2010 to 2025. Source: ScienceDirect (Data collected in July 2025).

Despite these breakthroughs, several challenges hinder the widespread adoption of N-CDs. To begin with, scalable synthesis methods with precise control over nitrogen content and configuration are still under development.<sup>15,16,20,21</sup> Second, long-term stability under diverse electrochemical conditions must be improved to ensure reliability in practical applications. Third, for combining N-CDs with complementary materials, including transparent metal oxides or conducting polymers, interfacial engineering needs to be improved. Finally, the large-scale production of N-CD is an environmental issue that would require newer, environmentally friendly methods of synthesis.<sup>22–26</sup>

This review presents a comprehensive and systematic analysis of recent advances in nitrogen-doped carbon dots (N-CDs) for electrochemical energy storage, emphasizing the connection between fundamental material properties and device-level performance. Unlike previous reviews, this work places a special emphasis on the structure–property–performance relationships dictated by nitrogen configuration and synthesis strategy, and it offers a critical techno-economic outlook essential for assessing commercial viability. The discussion begins with a systematic comparison of top-down and bottom-up synthesis strategies, linking precursor selection and functionalization to the resulting structural and chemical characteristics of N-CDs, followed by an exploration of advanced characterization techniques that reveal how nitrogen doping influences electronic conductivity, surface chemistry, and charge storage behavior. Mechanistic insights into the roles of various nitrogen types (pyridinic, pyrrolic, graphitic) and quantum confinement effects are provided to explain performance enhancements across devices. The review critically assesses N-CD applications in lithium-, sodium-, and potassium-ion batteries, supercapacitors, metal–air batteries, and hybrid systems, highlighting performance improvements and underlying mechanisms. It also explores N-CD-based nanocomposites with conductive polymers and metal compounds, underscoring their contributions to next-generation electrodes and solid-state electrolytes. The paper concludes with a forward-looking perspective on remaining challenges and research opportunities, integrating a techno-economic evaluation and discussing the roles of AI-guided design and sustainable synthesis in advancing high-performance, commercially viable N-CD-based energy storage technologies.

## 2 Synthesis strategies of N-CDs

The synthesis of N-CDs directly influences their physicochemical properties and electrochemical performance.<sup>27–31</sup> The two primary approaches for synthesizing N-CDs are the top-down and bottom-up methods,<sup>32,33</sup> as illustrated in Fig. 3.

### 2.1 Bottom-up approaches

In the bottom-up approach, small precursor molecules (*e.g.*, nitrogen-containing compounds like ammonia, ethylenediamine, or diethylenetriamine) are assembled into quantum dots through processes such as pyrolysis and carbonization<sup>34–36</sup> (Table 1).



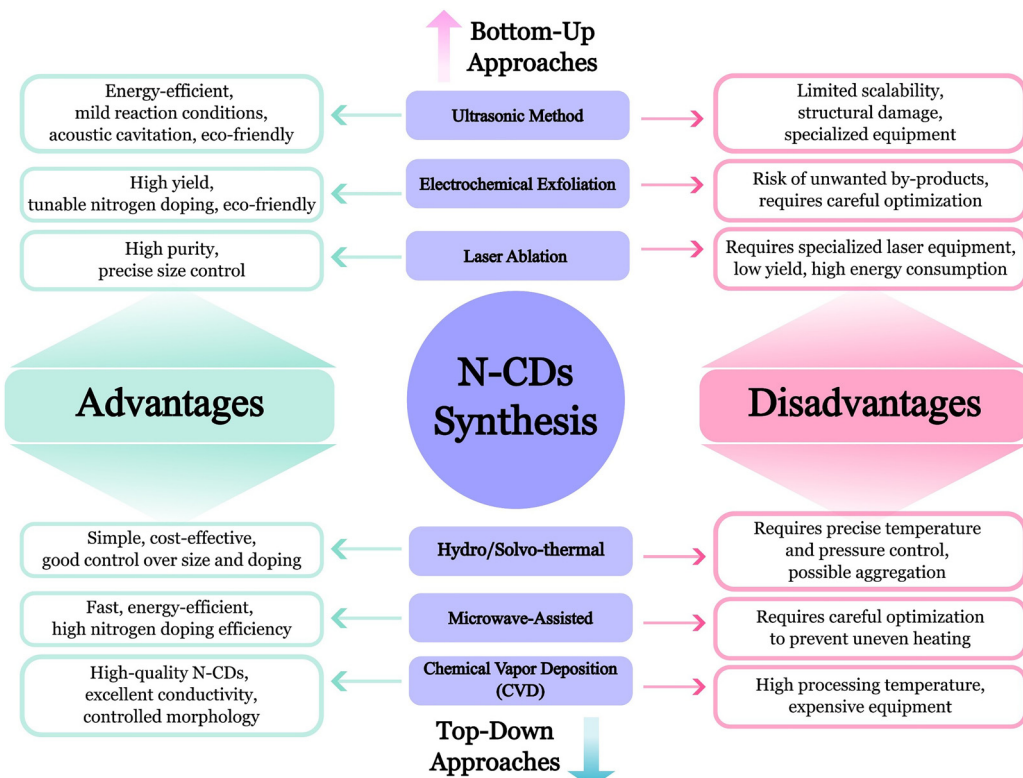


Fig. 3 Schematic comparison of top-down and bottom-up approaches for the synthesis of N-CDs.

This method also allows for nitrogen doping using organic waste or biomass.<sup>37</sup> Common techniques include:

**2.1.1 Solvothermal and hydrothermal methods.** Solvothermal and hydrothermal methods are among the most widely used techniques for synthesizing N-CDs. In these processes, organic precursors (*e.g.*, urea or ethylenediamine) are dissolved in water or a solvent, then subjected to high temperature and pressure, leading to carbonization and nitrogen doping. These methods are favored for their simplicity, cost-effectiveness, and ability to produce highly fluorescent and stable N-CDs.<sup>38</sup>

The versatility of this approach is evident in several studies. Xie *et al.*<sup>39</sup> developed an eco-friendly approach to synthesize N-CDs from highland barley *via* hydrothermal synthesis (Fig. 4).

In another investigation, Lei *et al.* introduced a simple solvothermal method to produce nitrogen-rich carbon quantum dots (CQDs) through spontaneous polymerization.<sup>40</sup> These CQDs exhibited exceptional electrocatalytic activity for the oxygen reduction reaction (ORR), making them valuable for energy conversion and storage (Fig. 5).

However, precise control over reaction conditions (precursor type, pressure, temperature, and duration) is crucial to tailor the size, morphology, and functional groups of N-CDs. For instance, longer reaction times and moderate temperatures enhance graphitization but may cause excessive aggregation, degrading electrochemical performance.<sup>41,42</sup>

**2.1.2 Microwave-assisted synthesis.** Microwave-assisted synthesis offers a rapid, scalable, and energy-efficient route for N-CD production. This method involves exposing precursor

solutions to microwave irradiation (typically 100–800 W) for short durations of 1–10 minutes, facilitating instantaneous heating that promotes both carbonization and nitrogen doping.<sup>43,44</sup> The technique provides distinct advantages over conventional approaches, including significantly reduced reaction times (minutes *versus* hours), exceptional nitrogen-doping efficiency, and lower energy requirements that make it environmentally favorable. A key benefit is the homogeneous heating profile generated by microwave irradiation, which ensures uniform particle size distribution and consistent product quality while minimizing thermal gradients common in traditional heating methods.<sup>45,46</sup>

Several studies demonstrate the versatility of this approach. Bhatt *et al.*<sup>47</sup> successfully employed microwave irradiation to synthesize N-CDs using prickly pear as a sustainable carbon source and *m*-xylylenediamine as nitrogen donor, achieving both cost-effectiveness and environmental benefits while producing CDs with enhanced fluorescence and surface functionality (Fig. 6).

In another study, Xiao *et al.* developed a streamlined single-step microwave process to generate highly photoluminescent nitrogen-enriched carbon dots, as illustrated in Fig. 7.<sup>48</sup> These investigations highlight how microwave-assisted methods can be adapted to different precursor systems while maintaining the technique's core advantages of speed, efficiency, and control over product characteristics.

**2.1.3 Chemical vapor deposition (CVD).** CVD is a versatile bottom-up approach for synthesizing high-quality N-CDs. In





Table 1 Precursor materials, synthesis methods, and applications of N-CDs

Research	Material sources	Methods	Key N-CDs properties	Applications	Ref.
Ma <i>et al.</i> (2012)		Glucose Ultrasonic	Small size (~3.5 nm), visible-light sensitive photocatalytic ability	Eco-friendly photocatalyst	78
Lei <i>et al.</i> (2016)		Ammonium hydroxide	Hydrothermal	High graphitic-N content, small size (~2 nm), bright fluorescence	40
T. Jebakumar Immanuel Edison <i>et al.</i> (2016)		N-methyl-2-pyrrolidone (NMP)		Bioimaging	79
Shouxin Liu <i>et al.</i> (2017)		β-alanine	Microwave-assisted synthesis	Small size (~4 nm), high quantum yield (~19%), low cytotoxicity	80
		L-ascorbic acid		Bioimaging	
		Microcrystalline Cellulose	Hydrothermal	High pyrrolic-N content, good dispersibility	
		Ethylenediamine		Environmental monitoring	



Table 1 (continued)

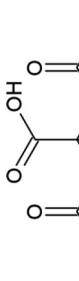
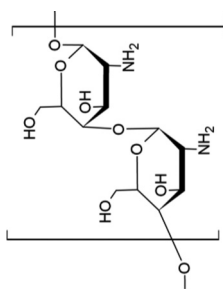
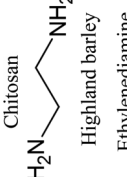
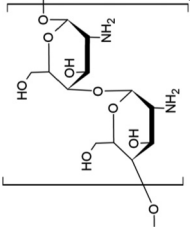
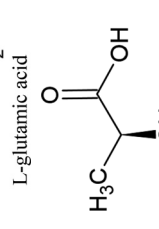
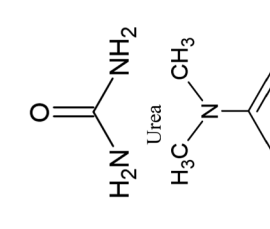
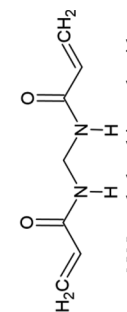
Research	Material sources	Methods	Key N-CDs properties	Applications	Ref.
Atchudana <i>et al.</i> (2017)	<i>C. retusa</i> fruit extract	Hydrothermal	Small size (~ 6.5 nm), spherical, low cytotoxicity	Metal ion sensing and biological applications	81
Xiao <i>et al.</i> (2017)		Microwave-assisted synthesis	High photoluminescence, nitrogen-rich content	Cellular imaging and multi-ion probing	48
Santiago <i>et al.</i> (2017)		Laser ablation	Controlled size, uniform morphology	Optoelectronic applications	64
					
Kumar <i>et al.</i> (2018)		CVD	High crystallinity, excellent electrical properties	Nano-optoelectronic applications	52
Xie <i>et al.</i> (2019)		Hydrothermal	Eco-friendly, high quantum yield, good recovery in real water samples	Detection of mercury ions ( $Hg^{2+}$ ) in aqueous solutions	39
Zhao <i>et al.</i> (2019)		Hydrothermal	Good biocompatibility, stable fluorescence, high pyridinic-N and pyrrolic-N content.	Fluorescent sensing of iron ions	82

Table 1 (continued)

Research	Material sources	Methods	Key N-CDs properties	Applications	Ref.
Ghanem <i>et al.</i> (2020)		Microwave-assisted synthesis	Ultra-small size (~1.5 nm), highly sensitive and selective “turn-off” sensor for $\text{Hg}^{2+}$ ions	Environmental monitoring	83
Shreya Bhatt <i>et al.</i> (2021)		Microwave-assisted synthesis	Small size (~6.5 nm), highly selective “on-off” sensor for Cr(VI)	Environmental sensing	47
Zhou <i>et al.</i> (2021)		Microwave-assisted synthesis	High pyrrolic-N/pyridinic-N content, effective copper corrosion inhibitor	Environmental sensing	73
Prickly pear		Electrochemical exfoliation			
Ammonium bicarbonate					
Glucose		Hydrothermal	Small size (~4 nm), rich in surface -COOH/-OH groups	Ion-detection and cell-imaging	84



Table 1 (continued)

Research	Material sources	Methods	Key N-CDs properties	Applications	Ref.
Monday <i>et al.</i> (2021)	Palm kernel shells	Hydrothermal and solvothermal	Small size (~4 nm), high pyridinic-N content	Biosensing	85
Qi <i>et al.</i> (2021)		Ultrasonic-assisted hydrothermal	Uniform size (~3.5 nm), excitation-dependent emission, low cytotoxicity	Cell imaging	86
Aydin <i>et al.</i> (2022)		Hydrothermal	Excitation-dependent emission, high pyrrolic-N content	Bioimaging	87
Liu <i>et al.</i> (2023)		Hydrothermal	Temperature-sensitive fluorescence	Temperature sensing	88
					

89

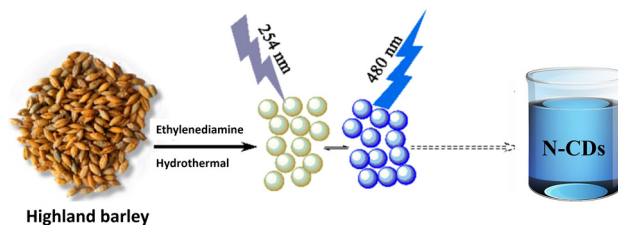
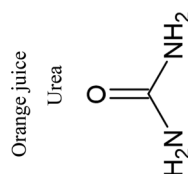


Fig. 4 Hydrothermal synthesis of N-CDs from highland barley.<sup>39</sup> Copyright 2019, MDPI.

Applications

Key N-CDs properties

Methods



Orange juice

Urea

Microwave-assisted synthesis

High quantum yield (~26.5%), small size (~3–6 nm), stable Fluorescent nano-sensing and cellular imaging

Ref.

Table 1 (continued)

Research	Material sources	Methods	Key N-CDs properties	Applications	Ref.
Galal Magdy <i>et al.</i> (2023)	Orange juice Urea	Microwave-assisted synthesis	High quantum yield (~26.5%), small size (~3–6 nm), stable Fluorescent nano-sensing and cellular imaging		

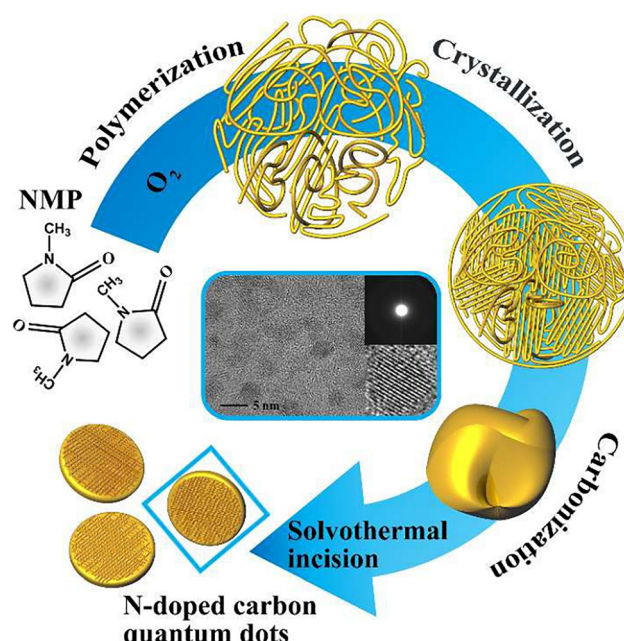


Fig. 5 One-step solvothermal synthesis of N-CDs from N-methylpyrrolidone (NMP).<sup>40</sup> Copyright 2016, Royal Society of Chemistry.

this process, hydrocarbon and nitrogen precursors are vaporized and decomposed at elevated temperatures (typically 500–1000 °C), facilitating the formation of carbon dots with controlled nitrogen incorporation.<sup>49</sup> The CVD technique enables precise tuning of doping concentrations, particle size, and graphitization degree, yielding N-CDs with exceptional electrical conductivity and well-defined surface characteristics.<sup>50,51</sup>

A notable application of this method was demonstrated by Kumar *et al.*,<sup>52</sup> who developed a one-step CVD synthesis of nitrogen-doped graphene quantum dots (N-GQDs) using



Fig. 6 Microwave-assisted synthesis of N-CDs from prickly pear and *m*-xylylenediamine.<sup>47</sup> Copyright 2021, Royal Society of Chemistry.



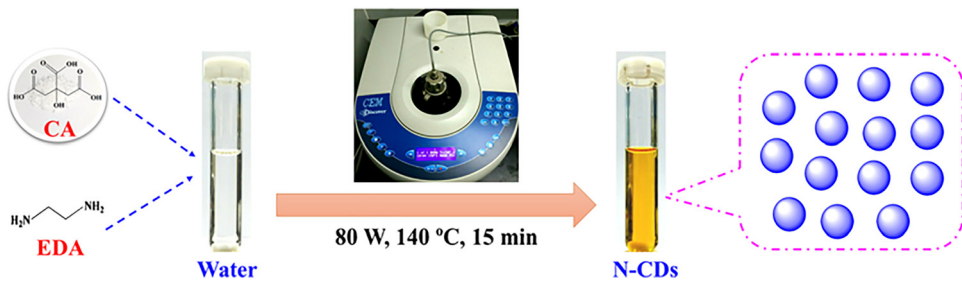


Fig. 7 Single-step microwave synthesis of photoluminescent N-CDs.<sup>48</sup> Copyright 2017, Springer.

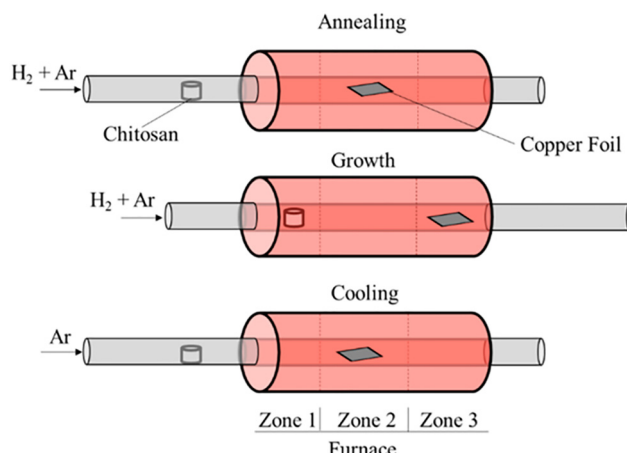


Fig. 8 Schematic illustration of the CVD synthesis process for N-GQDs.<sup>52</sup> Copyright 2018, American Chemical Society (ACS).

chitosan as a single precursor. This approach not only simplifies the fabrication process but also produces N-GQDs with outstanding optical and electronic properties (Fig. 8). The method represents an economically viable and scalable route for manufacturing high-performance nitrogen-doped quantum dots.

Despite these advantages, CVD faces limitations in large-scale energy storage applications due to its substantial energy demands from high-temperature operation and the need for sophisticated instrumentation. Additional challenges include the high capital cost of CVD systems and the stringent process control required for maintaining optimal gas flow rates and temperature profiles, which may hinder mass production.<sup>53</sup>

In summary, bottom-up approaches provide versatile routes for synthesizing N-CDs with tunable properties. While hydrothermal/solvothermal and microwave methods offer simplicity and efficiency for producing N-CDs with excellent electrochemical activity, techniques like CVD can yield highly graphitic, conductive N-CDs at the expense of scalability and cost. The choice of method is therefore a trade-off between the desired material quality, functionality, and practical considerations for large-scale energy storage applications.

## 2.2 Top-down approaches

Top-down approaches synthesize N-CDs by fragmenting bulk carbon materials into nanoscale particles<sup>29,54</sup> through physical,

chemical, or electrochemical processes (Table 1). In contrast to bottom-up methods that build N-CDs from molecular precursors, these techniques offer direct control over final particle size and composition, though typically require more energy-intensive processing. While effective for producing well-defined N-CDs, the inherent material waste and energy demands of size-reduction methods present significant challenges for scalable production.<sup>55–57</sup> Representative top-down methods include:

**2.2.1 Laser ablation.** Laser ablation has emerged as a precise top-down approach for synthesizing N-CDs with controlled size and surface properties. In this process, a high-energy laser irradiates a carbon target in a nitrogen-containing atmosphere, generating a plasma plume that facilitates the formation of N-CDs.<sup>58,59</sup> This technique yields high-purity N-CDs with well-defined morphology and uniform size distribution, making it particularly valuable for energy storage applications.

Recent studies have demonstrated the enhanced electrochemical performance of laser-ablated N-CDs in supercapacitor electrodes. When fabricated from graphite in nitrogen-rich environments and incorporated into composite electrodes, these N-CDs significantly improve charge transport and ion diffusion kinetics. The resulting supercapacitors exhibit exceptional specific capacitance and cycling stability, attributable to the optimized structural and electronic properties of the laser-synthesized N-CDs.<sup>60–63</sup>

Santiago *et al.*<sup>64</sup> advanced this methodology by developing pulsed laser ablation synthesis of N-GQDs using diethylenetriamine (DETA) as the nitrogen source. Their investigation revealed that this approach produces N-GQDs with remarkable photoluminescence properties (Fig. 9). The study provides valuable insights into the relationship between synthesis parameters and optical characteristics of the resulting quantum dots.

Despite its advantages, the widespread adoption of laser ablation faces practical challenges, including the need for specialized laser systems and substantial energy requirements. These factors currently limit the scalability of the technique for industrial-scale production.<sup>63,65</sup>

**2.2.2 Electrochemical exfoliation.** Electrochemical exfoliation represents a highly controllable and scalable top-down approach for synthesizing N-CDs. The method operates by applying a precisely tuned electric potential (typically 2–10 V) to a graphite electrode immersed in a nitrogen-containing electrolyte solution, often comprising ammonium salts or organic amines. During this process, three concurrent phenomena occur: (1) electrochemical



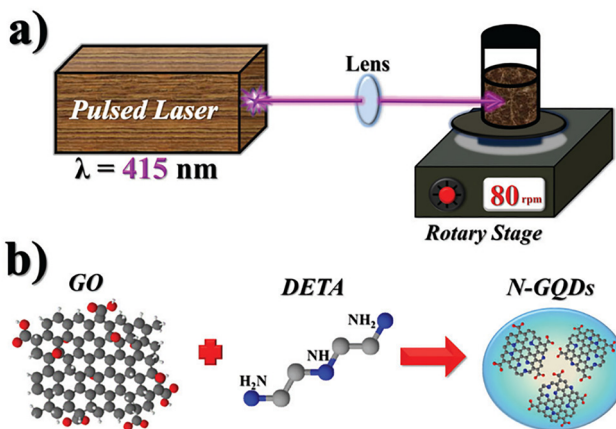


Fig. 9 Schematic illustration of (a) the pulsed laser ablation setup for N-GQD synthesis and (b) the DETA-mediated N-GQD formation process.<sup>64</sup> Copyright 2017, Royal Society of Chemistry.

oxidation of the graphite surface, (2) intercalation of electrolyte ions between graphene layers, and (3) gas evolution from electrolyte decomposition. These combined effects lead to the progressive exfoliation of carbon sheets and their subsequent fragmentation into nanoscale carbon dots, while dissolved nitrogen species become incorporated into the evolving carbon matrix.<sup>66–68</sup>

The technique's exceptional tunability stems from multiple adjustable parameters. Applied voltage directly controls the exfoliation rate and defect density, while electrolyte composition determines both the nitrogen doping mechanism (typically yielding 2–15 at% nitrogen content) and the resulting surface functional groups. Reaction duration (ranging from minutes to hours) further influences the final particle size distribution (commonly 2–10 nm) and crystallinity. This parameter space enables researchers to precisely engineer N-CDs with tailored optoelectronic properties for specific applications.<sup>69,70</sup>

From a production standpoint, electrochemical exfoliation offers significant advantages over other top-down methods. The process occurs at moderate temperatures (20–80 °C) without requiring expensive vacuum systems or high-power lasers, making it both energy-efficient and cost-effective for industrial-scale implementation. The aqueous-based chemistry minimizes environmental impact while achieving impressive production yields exceeding 60%. These practical benefits combine with the intrinsic material advantages of nitrogen doping, which

introduces n-type charge carriers, creates catalytically active sites, and improves electrode–electrolyte interactions through enhanced surface wettability.<sup>67,70–72</sup>

Zhou *et al.*<sup>73</sup> demonstrated the industrial potential of this approach through their optimized electrochemical synthesis of N-CQDs. Their systematic investigation revealed how careful control of electrochemical parameters could produce gram-scale quantities of N-CQDs with uniform size distribution and optimal nitrogen configuration (predominantly graphitic and pyridinic N species). The resulting materials showed exceptional performance in energy storage devices, attributable to their balanced combination of high conductivity, abundant active sites, and structural stability (Fig. 10).

**2.2.3 Ultrasonic synthesis method.** The ultrasonic method has emerged as an efficient top-down approach for synthesizing N-CDs, leveraging high-frequency sound waves (>20 kHz) to achieve nanoparticle formation, functionalization, and dispersion. This sonochemical process relies on acoustic cavitation, where ultrasonic waves generate microscopic bubbles in the reaction medium that undergo rapid formation, growth, and violent collapse.<sup>54,55</sup> The transient collapse of these bubbles creates localized extreme conditions (temperatures  $\sim$  5000 K and pressures  $\sim$  1000 atm) that drive two critical processes: (1) pyrolysis of organic precursors into carbonaceous fragments and (2) incorporation of nitrogen species into the evolving carbon matrix.<sup>74,75</sup>

Compared to conventional synthesis methods, ultrasonic processing offers distinct advantages for N-CD production. The technique operates at ambient conditions without requiring high temperatures or pressures, making it both energy-efficient and environmentally benign. The intense micro-mixing generated by cavitation ensures homogeneous dispersion of nanoparticles while preventing aggregation through continuous disruption of intermolecular forces. Furthermore, the method provides excellent control over particle size (typically 2–8 nm) and surface functionality through adjustment of ultrasonic parameters, including frequency (20–1000 kHz), power density (10–500 W cm<sup>-2</sup>), and processing time (minutes to hours).<sup>74,76,77</sup>

Ma *et al.*<sup>78</sup> demonstrated the effectiveness of this approach through their innovative one-step ultrasonic synthesis of N-CDs from glucose precursors. Their optimized protocol produced photocatalytically active N-CDs with excellent visible-light responsiveness, as illustrated in Fig. 11. The study highlighted

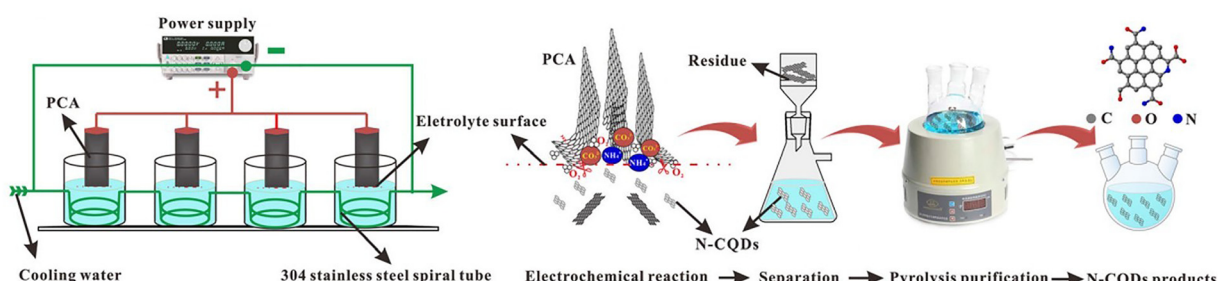


Fig. 10 Schematic depiction of the electrochemical exfoliation apparatus for the N-CQDs-related experimental device.<sup>73</sup> Copyright 2021, Springer.

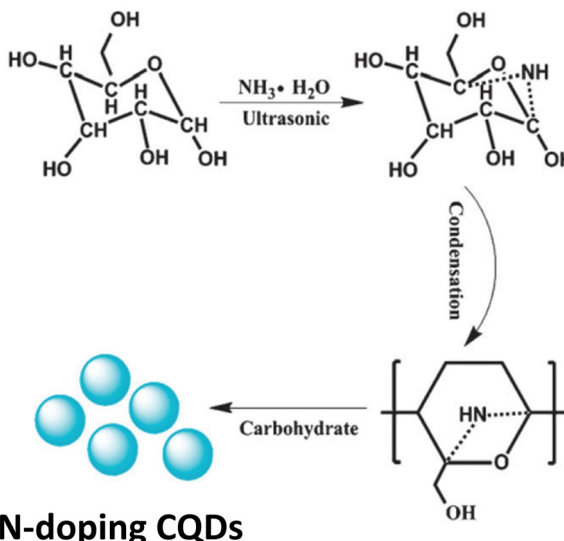
**N-doping CQDs**

Fig. 11 Schematic representation of the ultrasonic synthesis process for N-CDs from glucose precursors.<sup>78</sup> Copyright 2012, Royal Society of Chemistry.

how ultrasonic parameters could be tuned to control the nitrogen doping configuration (primarily pyridinic and pyrrolic N) and optical properties of the resulting carbon dots.

In summary, top-down approaches provide an alternative pathway to N-CDs by fragmenting bulk carbon sources, offering direct control over particle size and composition. While methods like laser ablation and electrochemical exfoliation can produce high-quality N-CDs with uniform morphology and competitive electrochemical performance, these techniques are generally characterized by higher energy consumption and lower material yield compared to bottom-up routes. This inherent trade-off between precise material control and

scalable, cost-effective production currently limits the widespread industrial adoption of top-down methods for energy storage applications.

### 2.3 Precursor selection and its impact on N-doping

The choice of molecular precursors fundamentally determines the nitrogen doping efficiency and resulting properties of N-CDs.<sup>90</sup> Nitrogen-rich compounds containing amines, amides, or heterocyclic structures serve as particularly effective precursors, enabling high doping levels that enhance electrical conductivity, surface polarity, and electrocatalytic activity (Fig. 12). The molecular architecture of these precursors directly influences three critical structural parameters: (1) degree of graphitization, (2) pore volume distribution, and (3) specific surface area—all of which collectively govern ion diffusion kinetics and charge storage capacity.<sup>91–93</sup>

Precursor selection follows distinct structure–property relationships. Aromatic precursors like aniline or pyridine typically yield N-CDs with higher graphitization degrees and superior electrical conductivity due to their inherent conjugated systems. In contrast, aliphatic precursors such as ethylenediamine tend to produce less graphitic but more surface-reactive structures with abundant edge sites.<sup>90,94,95</sup> This precursor-dependent behavior necessitates careful optimization for energy storage applications, where both bulk and surface properties must be balanced through strategic precursor selection and post-synthetic modifications.<sup>91,96</sup>

The thermal processing parameters further modulate nitrogen incorporation. Lower pyrolysis temperatures predominantly preserve pyridinic and pyrrolic nitrogen configurations, while higher temperatures favor graphitic nitrogen formation at the expense of overall nitrogen content through volatile loss.<sup>97</sup> This temperature-dependent nitrogen speciation creates an optimization challenge—higher processing temperatures improve electrical conductivity

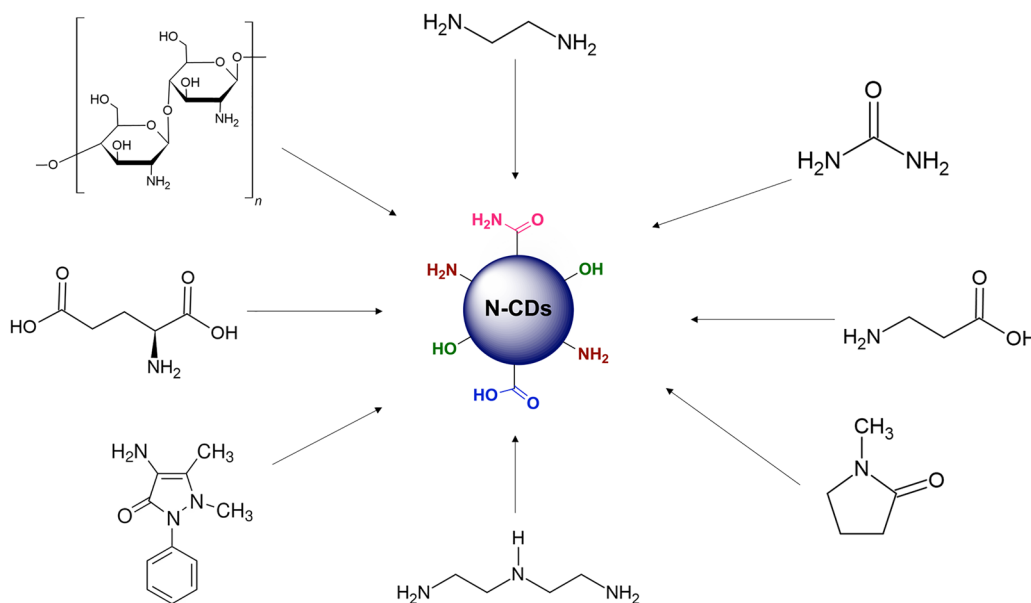


Fig. 12 A graphical illustration of typical N-CD starting materials.



but reduce accessible active sites, requiring careful balancing for specific applications.<sup>96,98</sup>

#### 2.4 Functionalization strategies for enhanced electrochemical performance

Controlled functionalization of N-CDs serves as a powerful approach to optimize their electrochemical performance. The introduction of oxygen-containing groups (hydroxyl, carboxyl) or nitrogen-based functionalities (amine, amide) significantly enhances surface wettability and electrolyte accessibility, thereby improving ion transport kinetics in energy storage devices (Fig. 13).<sup>94</sup> More importantly, co-doping with secondary heteroatoms (sulfur, phosphorus, boron) creates synergistic effects that further boost charge transfer capabilities, catalytic activity, and cycling stability.<sup>99,100</sup>

Particularly noteworthy is the sulfur–nitrogen dual-doping strategy, which generates additional redox-active sites while maintaining good conductivity. Such S,N-co-doped CDs demonstrate exceptional pseudocapacitive behavior in supercapacitor applications, often doubling or tripling the specific capacitance compared to singly-doped counterparts. Similarly, constructing hybrid architectures by combining N-CDs with conductive polymers (polyaniline, polypyrrole) or metal oxides ( $MnO_2$ ,  $RuO_2$ ) through *in situ* growth or post-synthetic modification can substantially enhance both stability and electrochemical activity.<sup>94,99–101</sup>

### 3 Structural characterization and physicochemical properties of N-CDs

Energy storage applications depend critically on the structural and physicochemical properties of N-CDs. Key factors, such as chemical composition, optical properties, electrical

conductivity, and surface/electrochemical stability, directly influence charge transfer kinetics, ion mobility, and overall storage efficiency.<sup>94</sup> The unique structure of N-CDs, characterized by their small size, high surface area, tunable functional groups, and nitrogen incorporation, enhances their electrochemical performance.<sup>100,102</sup> This section discusses the essential properties of N-CDs and their implications for energy storage devices. Fig. 14 illustrates the characterization techniques and structural features used to analyze N-CDs.

#### 3.1 Chemical composition and functional groups

The chemical composition of N-CDs is predominantly governed by their synthetic precursors and reaction conditions, with carbon, nitrogen, hydrogen, and oxygen as the primary constituent elements. Nitrogen incorporation into the graphene-like framework significantly enhances electronic conductivity and electrochemical reactivity through the formation of pyridinic-N, pyrrolic-N, and graphitic-N configurations.<sup>37,38</sup> Among these, pyridinic-N and pyrrolic-N actively participate in charge transfer and redox reactions, while graphitic-N, embedded within the carbon matrix, improves overall electrical conductivity.<sup>103</sup> Furthermore, the presence of oxidized nitrogen species introduces a negative surface charge, which facilitates enhanced ion adsorption.<sup>104</sup>

The surface of N-CDs is typically functionalized with amine ( $-NH_2$ ), carboxyl ( $-COOH$ ), and hydroxyl ( $-OH$ ) groups, which collectively improve the material's solubility, dispersibility, and interfacial interactions with electrodes. These functional groups also contribute to pseudocapacitive behavior through reversible ion adsorption and redox processes.<sup>105</sup> To thoroughly characterize these chemical and structural features, advanced analytical techniques such as Fourier-transform infrared spectroscopy (FTIR), X-ray photoelectron spectroscopy (XPS),

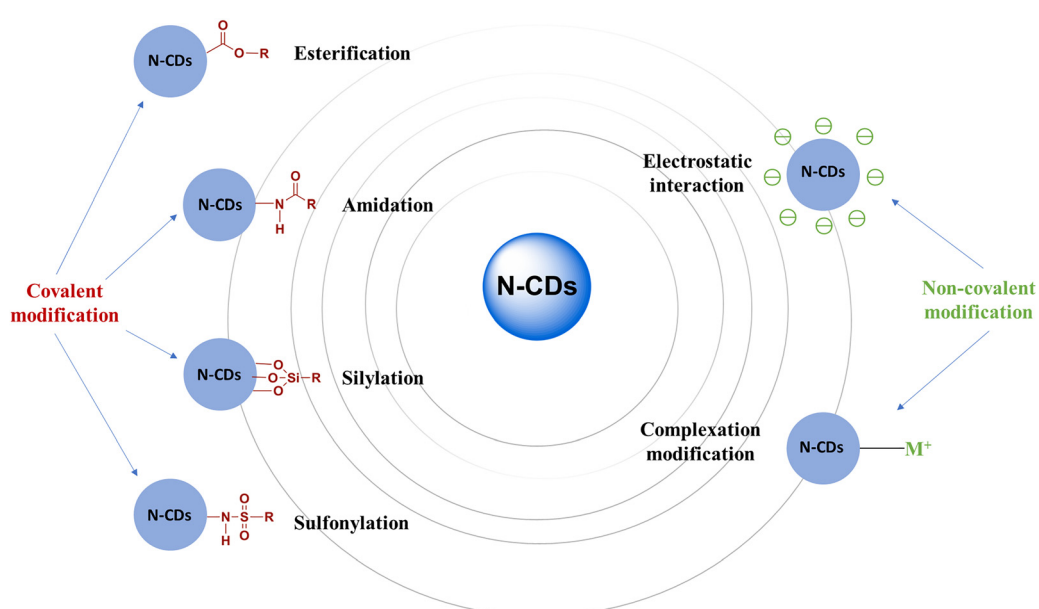


Fig. 13 Schematic illustration of common surface modification strategies for N-CDs.



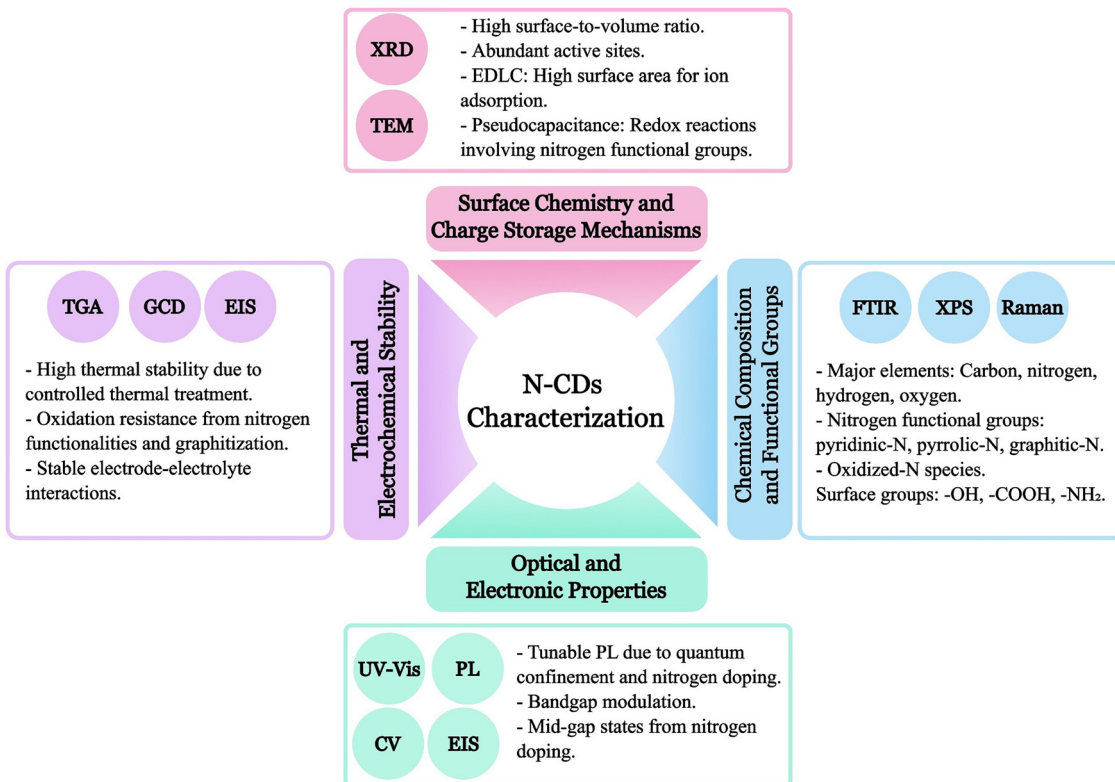


Fig. 14 Characterization techniques and structural features of N-CDs.

Raman spectroscopy, and X-ray diffraction (XRD) are routinely employed.

Nelson *et al.* conducted a detailed structural analysis of synthesized N-CDs using XRD and Raman spectroscopy.<sup>106</sup> The XRD pattern (Fig. 15a) exhibited a broad diffraction peak centered at 26°, characteristic of an amorphous graphitic carbon structure. Complementary Raman spectra (Fig. 15b) revealed two distinct bands at approximately 1350 cm<sup>-1</sup> (D band) and 1580 cm<sup>-1</sup> (G band), indicative of disordered carbon domains and graphitic ordering, respectively. These findings confirm the hybrid structural nature of N-CDs, comprising both crystalline and amorphous regions.

In a separate study, Kamaraj *et al.*<sup>107</sup> utilized FTIR spectroscopy to probe the surface functional groups of N-CDs. The FTIR spectrum (Fig. 16) displayed prominent absorption bands corresponding to O-H/N-H stretching vibrations (3400 cm<sup>-1</sup>), C=O carbonyl stretching (1720 cm<sup>-1</sup>), and C-N/C-O bond vibrations (1200–1300 cm<sup>-1</sup>), providing clear evidence of oxygen- and nitrogen-containing surface functionalities.

Lei *et al.*<sup>40</sup> further investigated the surface chemistry of N-CDs through XPS analysis (Fig. 17). The survey scan confirmed the presence of carbon, nitrogen, and oxygen as the primary elements. High-resolution C 1s spectra deconvoluted into three components: C-C/C=C (sp<sup>2</sup> carbon), C-N (nitrogen-doped

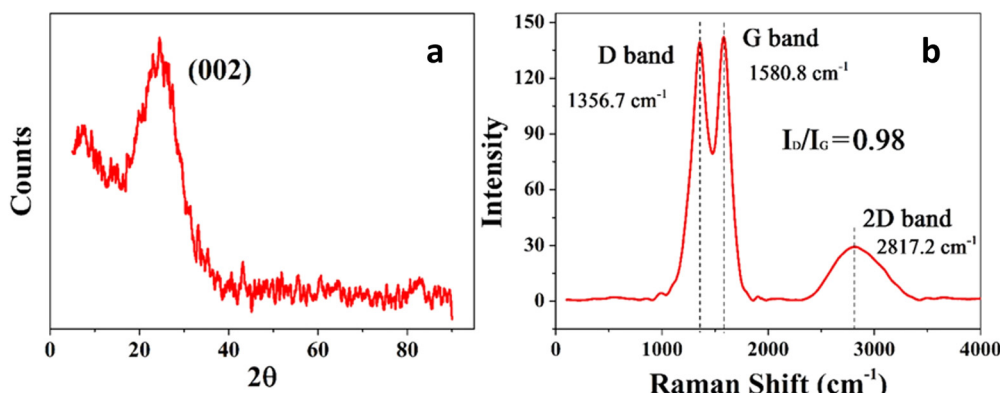


Fig. 15 (a) XRD pattern and (b) Raman spectrum of N-CDs.<sup>106</sup> Copyright 2025, Springer.



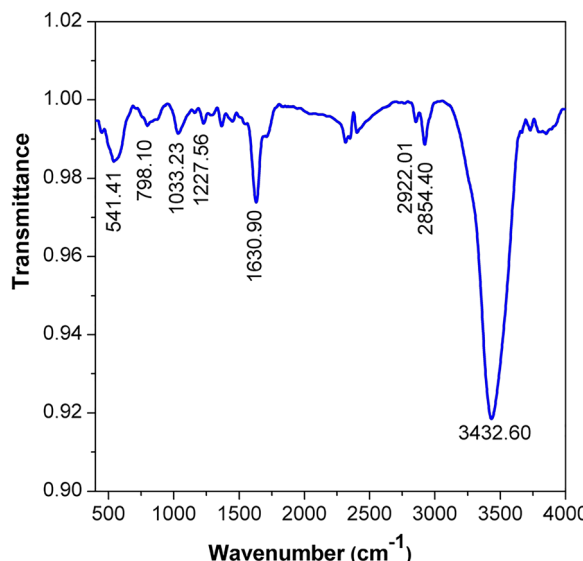


Fig. 16 FTIR spectrum of N-CDs.<sup>107</sup> Copyright 2025, Chemistry Europe.

carbon), and C=O (carbonyl groups). The N 1s spectrum resolved contributions from pyrrolic-N, graphitic-N, and amine-type nitrogen, demonstrating successful nitrogen doping. Additionally, the O 1s spectrum revealed oxygen species in hydroxyl and carbonyl environments, further corroborating the presence of oxygenated surface groups.

Collectively, the literature confirms that advanced characterization techniques (XPS, FTIR, Raman, XRD) are indispensable for linking synthesis to performance. They consistently demonstrate that successful nitrogen doping, achieving a balance of pyridinic-N for redox activity, pyrrolic-N for electrolyte interaction, and graphitic-N for conductivity, is the cornerstone of enhancing the electrochemical functionality of N-CDs.

### 3.2 Optical and electronic properties

N-CDs possess distinctive optical and electronic characteristics arising from quantum confinement effects and nitrogen doping, which collectively govern their photoluminescence behavior and electronic structure. The tunable photoluminescence emission, which can be precisely controlled through synthesis parameters, renders N-CDs particularly valuable for optoelectronic and sensing applications. For energy storage systems, their electronic properties, including bandgap modulation and enhanced conductivity, are of paramount importance. The incorporation of nitrogen atoms creates mid-gap states near the Fermi level, significantly improving charge carrier mobility and electrochemical activity.<sup>41,46,49,58,62,85,94</sup> In particular, pyridinic-N and pyrrolic-N configurations introduce localized states that enhance redox activity, while graphitic-N species extend  $\pi$ -conjugation networks to boost electrical conductivity.<sup>103,108</sup>

Researchers commonly employ UV-vis absorption and photoluminescence spectroscopy (PL) to investigate the electronic transition behaviors of N-CDs, while electrochemical

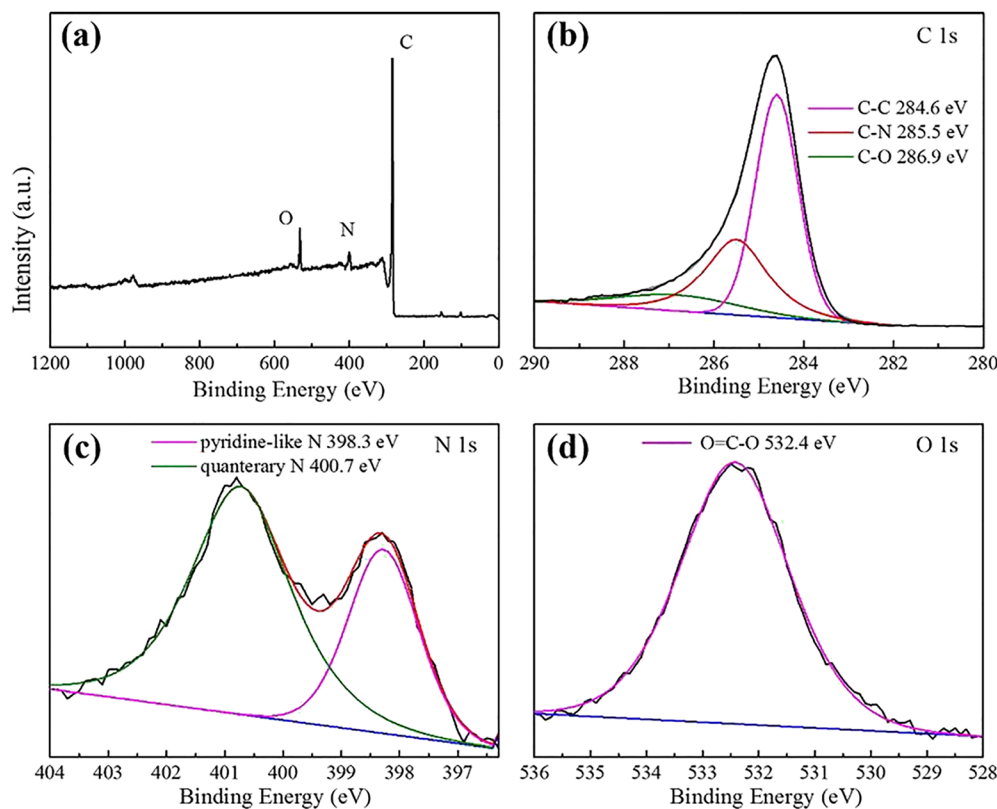
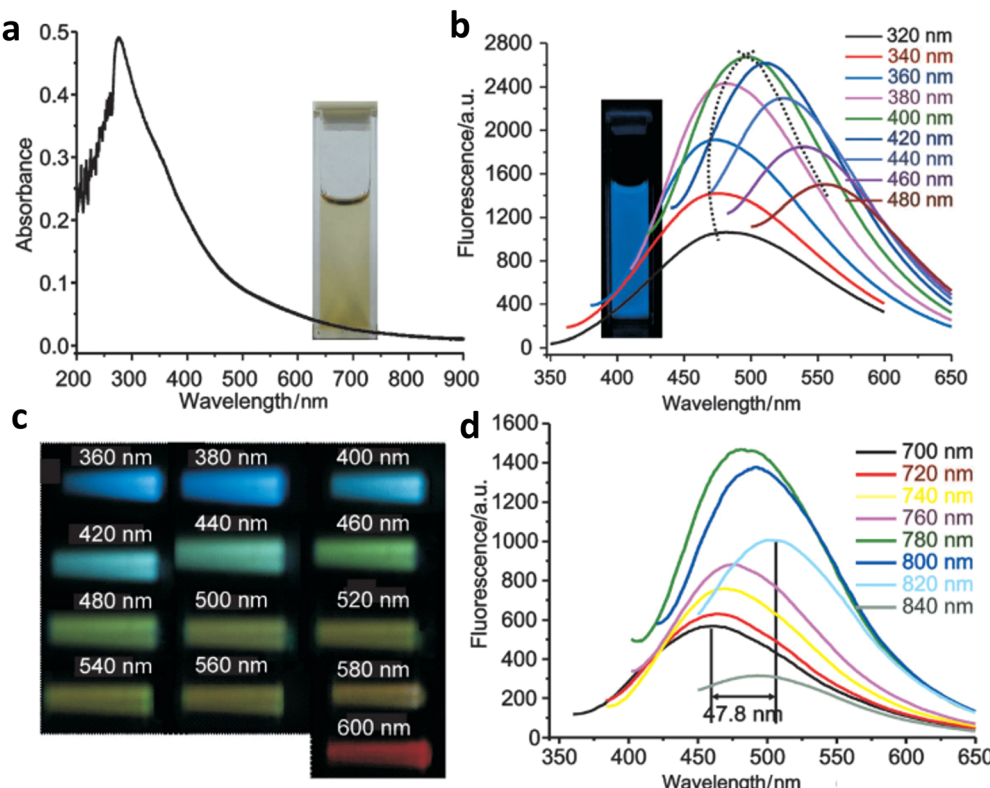


Fig. 17 XPS analysis of N-CDs annealed at 800 °C: (a) survey scan confirming C/N/O presence, (b) detailed C 1s spectrum, (c) high-resolution N 1s signal, and (d) O 1s peak analysis.<sup>40</sup> Copyright 2016, Royal Society of Chemistry.





**Fig. 18** (a) UV-Vis absorption spectra of N-CDs with an inset showing solution appearance. (b) Excitation-dependent photoluminescence spectra featuring inset emission under 380 nm excitation. (c) Fluorescence microscopy images captured at different excitation wavelengths. (d) Up conversion photoluminescence spectra demonstrating anti-Stokes emission properties.<sup>109</sup> Copyright 2013, Wiley.

techniques such as cyclic voltammetry (CV) and electrochemical impedance spectroscopy (EIS) provide critical insights into their charge transport efficiency.<sup>85</sup>

Yang *et al.*<sup>109</sup> conducted a comprehensive optical characterization of N-CDs using UV-vis absorption spectroscopy, revealing distinct electronic transitions as shown in Fig. 18a. Their studies also demonstrated excitation-dependent photoluminescence behavior (Fig. 18b), with additional confirmation through fluorescence microscopy imaging under various excitation wavelengths (Fig. 18c). Notably, the observed upconversion photoluminescence characteristics (Fig. 18d) suggest potential applications requiring anti-Stokes shift phenomena.

### 3.3 Surface chemistry and charge storage mechanisms

The surface chemistry of N-CDs plays a pivotal role in their charge storage performance by governing ion adsorption, charge transport kinetics, and electrochemical stability. Their nanoscale size and high surface-to-volume ratio provide abundant active sites for charge accumulation, making them highly effective for capacitive energy storage.<sup>102,110-112</sup>

N-CDs exhibit a dual charge storage mechanism, combining electric double-layer capacitance (EDLC) and pseudocapacitance. In EDLC, their large surface area facilitates rapid electrolyte ion adsorption, forming a stable electric double layer at the electrode–electrolyte interface.<sup>113</sup> This process is further enhanced by graphitic nitrogen doping, which improves

electrical conductivity and enables ultrafast charge/discharge cycles.<sup>35,114</sup> Additionally, heteroatom doping (e.g., sulfur, boron, phosphorus) or hybridization with graphene/metal oxides can further boost performance by introducing additional active sites and improving electron transfer.<sup>112</sup>

The structural and porosity characteristics of N-CDs, which directly influence their charge storage behavior, are typically analyzed using transmission electron microscopy (TEM) and X-ray diffraction (XRD). For instance, He *et al.*<sup>44</sup> systematically investigated the size-dependent properties of N-CDs synthesized under different conditions (Fig. 19). N-CDs prepared at 160 °C (N-CDs160-1) showed a relatively large particle size (~4.31 nm), attributed to loosely packed polymer clusters (Fig. 19a and b). When the temperature was increased to 200 °C (N-CDs200-1), the particle size decreased significantly (~1.05 nm) due to enhanced carbon core formation *via* dehydration and carbonization (Fig. 19c and d). Prolonged reaction time led to larger carbon cores, with N-CDs 200-2 exhibiting an intermediate size of ~2.24 nm (Fig. 19e and f).

### 3.4 Thermal and electrochemical stability

The thermal and electrochemical stability of N-CDs represents a critical factor determining their practical utility in energy storage applications. When synthesized through controlled thermal treatment processes, N-CDs demonstrate remarkable thermal stability that enables their operation in high-



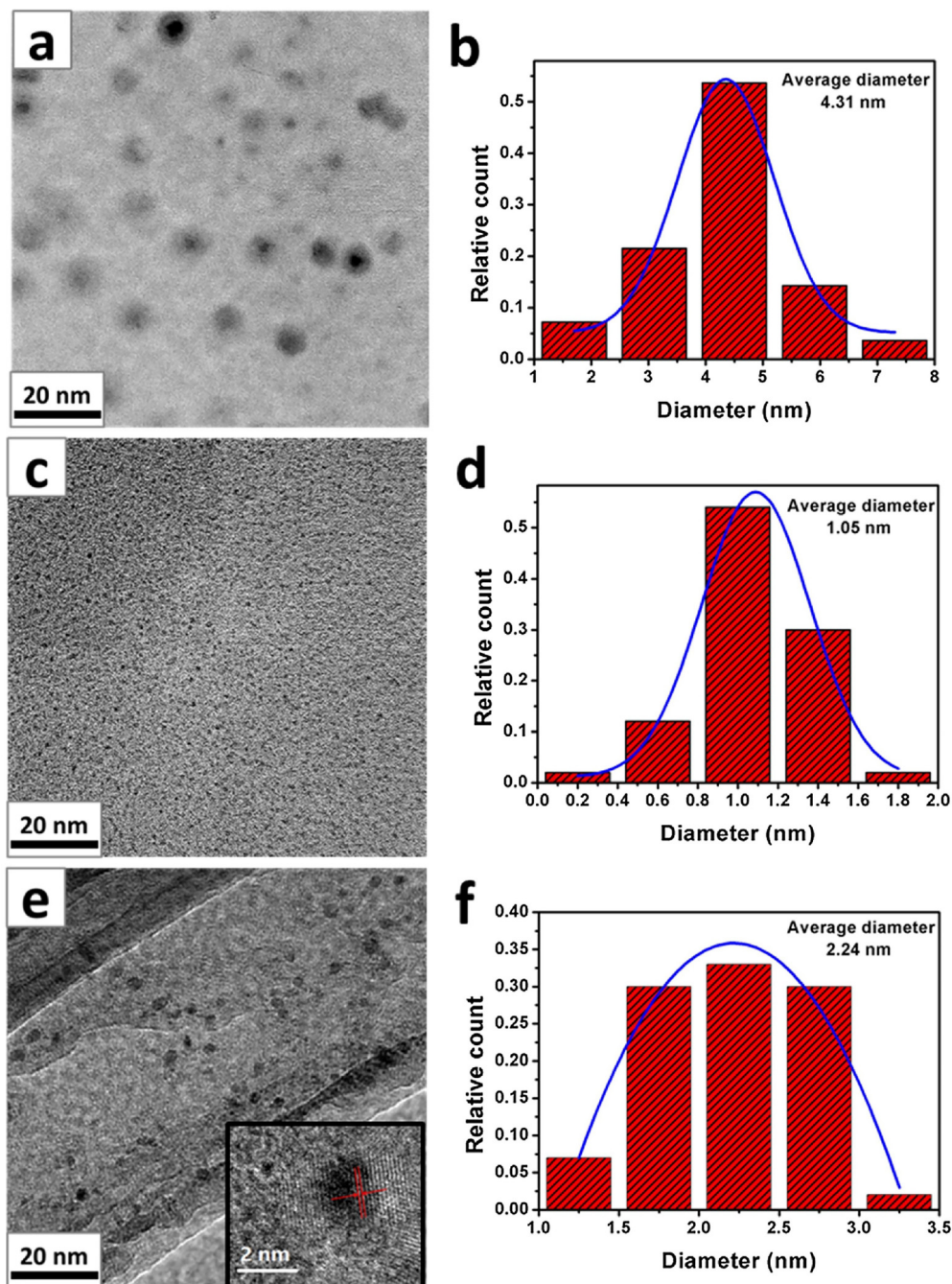


Fig. 19 TEM images and corresponding particle size distributions of (a) and (b) N-CDs160-1, (c) and (d) N-CDs200-1, and (e) and (f) N-CDs200-2.<sup>44</sup> Copyright 2017, Elsevier.

temperature environments. Researchers commonly employ thermogravimetric analysis (TGA) to systematically evaluate the thermal degradation behavior of these materials, providing valuable insights into their structural robustness under thermal stress. From an electrochemical perspective, the stability of N-CDs primarily depends on two key structural characteristics: the nature of nitrogen functional groups and the degree of graphitization. Stable nitrogen configurations such as pyridinic-N and graphitic-N significantly enhance oxidation resistance while maintaining redox activity, whereas a high degree of

graphitization contributes to superior structural integrity during prolonged cycling.<sup>115,116</sup> These features collectively enable N-CDs to maintain their electrochemical capacity over extended charge-discharge operations. Furthermore, the operational electrolyte environment, whether acidic, neutral, or alkaline, plays a crucial role in determining the redox behavior and overall charge storage efficiency of these materials.<sup>68</sup> Standard electrochemical characterization techniques, including galvanostatic charge-discharge (GCD) testing and electrochemical impedance spectroscopy (EIS), provide essential data for evaluating long-term cycling performance and stability.

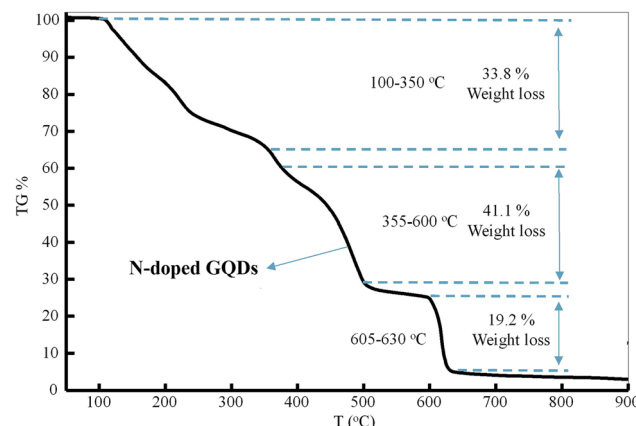


Fig. 20 TGA curve showing the thermal decomposition profile of N-doped GQDs.<sup>117</sup> Copyright 2019, Elsevier.

A representative study by Senel *et al.*<sup>117</sup> investigated the thermal properties of nitrogen-doped graphene quantum dots (N-doped GQDs) using TGA. Their analysis revealed distinct thermal decomposition stages, beginning with an initial weight loss below 150 °C corresponding to the evaporation of adsorbed water molecules and volatile residues. The subsequent significant mass loss occurring between 200–400 °C was attributed to the thermal decomposition of oxygen-containing surface functional groups such as hydroxyl and carboxyl moieties. This thermal behavior profile not only confirms the material's substantial surface functionalization but also highlights its potential for applications requiring hydrophilic and biocompatible properties. The TGA data, presented in Fig. 20, provide clear evidence of these thermal characteristics.

## 4 Mechanistic insights into the role of N-CDs in energy storage

N-CDs significantly enhance energy storage performance by tailoring electronic properties, enabling efficient charge transfer and synergistic interactions with electroactive materials<sup>118,119</sup> (Fig. 21). These improvements are driven by nitrogen doping, quantum confinement effects, and interfacial dynamics, which collectively optimize electrochemical behavior. Understanding such mechanisms, particularly in supercapacitors and batteries, is critical for advancing current systems and designing next-generation high-efficiency devices.<sup>120,121</sup>

### 4.1 Nitrogen-doping and its effect on electronic conductivity

Nitrogen doping enhances the electron conductivity of carbon dots by introducing additional charge carriers and modifying the density of states near the Fermi level.<sup>122</sup> Nitrogen incorporation alters the electronic structure, promoting  $\pi$ -electron delocalization and enhancing charge carrier mobility.<sup>123</sup> The high conductivity of N-CDs facilitates rapid electron transfer during electrochemical reactions, making them ideal for energy storage devices.<sup>124</sup> Additionally, nitrogen doping creates defects and active sites that enable pseudocapacitive behavior, supporting reversible surface reactions.<sup>125</sup> Pyridinic-N contributes edge-localized lone-pair electrons, enhancing charge storage and redox activity, while pyrrolic-N participates in reversible redox reactions.<sup>126,127</sup> Owing to their superior conductivity and electrochemical activity, N-CDs enable faster charge/discharge cycles in supercapacitors and lithium-ion batteries.<sup>128</sup> Techniques such as XPS and Raman spectroscopy are widely used to probe nitrogen's influence on the electronic properties of N-CDs.<sup>129</sup>

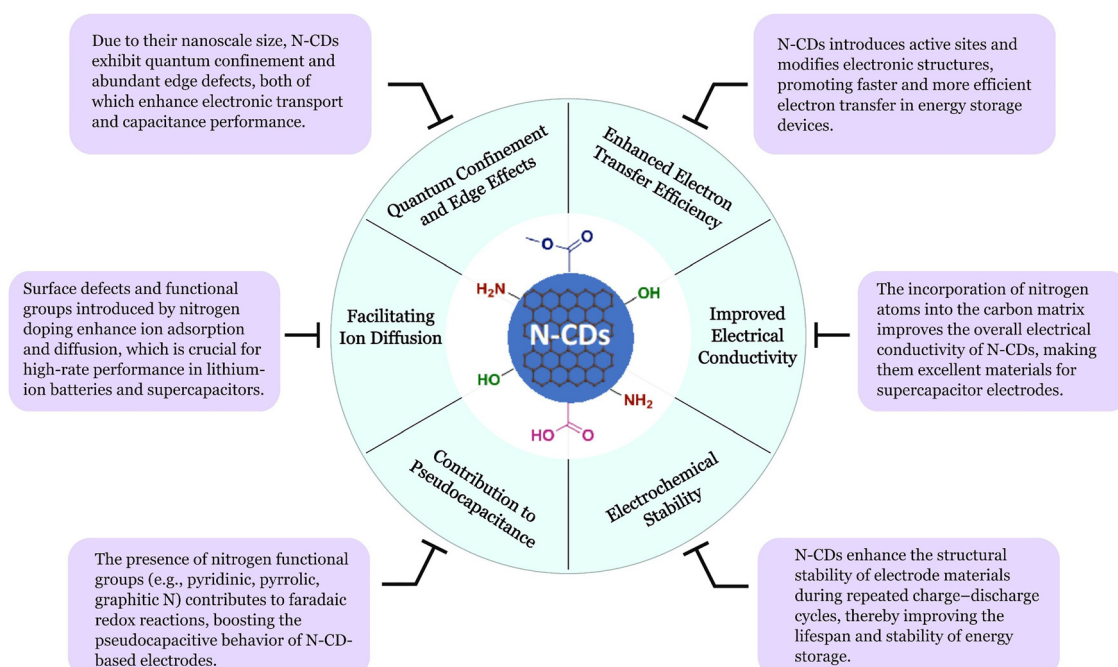


Fig. 21 Schematic diagram of the role of N-CDs in energy storage.



## 4.2 Quantum confinement and enhanced charge transfer

The nanoscale size of N-CDs induces quantum confinement, enhancing their charge storage and transfer efficiency.<sup>130</sup> Quantum confinement modifies electronic band structures, promoting charge separation, accelerating electron mobility, and suppressing recombination.<sup>131,132</sup> Their high surface-to-volume ratio facilitates greater ion and charge transport. Nitrogen doping further enhances these effects by creating charge-trapping sites, improving charge retention.<sup>131</sup> This reduces recombination losses, stabilizes charge flow, and improves energy storage efficiency.<sup>132</sup> In supercapacitors, quantum confinement improves electric double-layer capacitance (EDLC) by increasing the electroactive surface area for ion adsorption. In batteries, it enhances ion diffusion kinetics, enabling faster charge/discharge rates and higher energy density.<sup>132,133</sup>

## 4.3 Synergistic interactions with other electroactive materials

N-CDs synergize with electroactive materials (*e.g.*, transition metal oxides, conductive polymers, and carbon-based nanomaterials) to significantly enhance energy storage performance.<sup>124,134,135</sup> These interactions optimize charge transfer kinetics, increase capacitance, and improve electrochemical stability.<sup>124</sup> For example, in graphene-based composites, N-CDs prevent graphene restacking, expanding the electroactive surface area for ion adsorption while acting as conductive bridges between sheets. In hybrid systems with metal oxides (*e.g.*, TiO<sub>2</sub>, MnO<sub>2</sub>, Fe<sub>2</sub>O<sub>3</sub>), N-CDs lower charge transfer resistance and enhance redox activity. Their high dispersibility and surface functional groups promote uniform integration, optimizing electrode performance. Such synergies make N-CD composites ideal for next-generation energy storage, delivering high capacitance, fast charge/discharge rates, and exceptional cycling stability.<sup>136,137</sup>

## 4.4 Influence of doping type (pyridinic, pyrrolic, graphitic nitrogen) on performance

The electrochemical performance of N-CDs is strongly influenced by their nitrogen configurations: pyridinic, pyrrolic, and graphitic nitrogen. Pyridinic nitrogen, located at the edges of the carbon lattice, enhances redox reactions and pseudocapacitance by donating lone-pair electrons.<sup>138</sup> Pyrrolic nitrogen, incorporated into five-membered rings, boosts charge storage capacity and improves electrolyte wettability, enhancing ion diffusion.<sup>139,140</sup> Graphitic nitrogen, embedded within the carbon lattice, enhances electrical conductivity and cycling stability by facilitating electron delocalization.<sup>37</sup> The electrochemical properties of N-CDs can be tailored by optimizing synthesis parameters, including precursor selection and reaction conditions.<sup>124,138</sup> Through precise control, N-CDs can be engineered for high charge capacity, rapid charge/discharge kinetics, and long-term cycling stability.<sup>139</sup>

# 5 Applications of N-CDs in energy storage devices

N-CDs have emerged as versatile components for advanced energy storage systems, owing to their high electrical

conductivity, tunable surface chemistry, and remarkable electrochemical activity. They have been successfully integrated into various energy storage devices, including supercapacitors, lithium-ion batteries (LIBs), sodium-ion batteries (SIBs), potassium-ion batteries (PIBs), metal-air batteries, and hybrid systems (Fig. 22).<sup>141–143</sup> N-CDs serve multiple functional roles, as summarized in Table 2.

Furthermore, Table 3 presents a quantitative overview of the performance enhancements achieved by incorporating N-CDs into these systems. This section critically analyzes these applications, emphasizing the underlying mechanisms and specific roles through which N-CDs contribute to improved electrochemical performance.<sup>159,160</sup>

## 5.1 Supercapacitors

Supercapacitors (electrochemical capacitors) store energy through electrical double-layer capacitance (EDLC) and pseudocapacitive mechanisms.<sup>162</sup> While carbon-based materials traditionally dominate EDLC-dominated devices, their performance is often limited by moderate specific energy.<sup>169</sup> The integration of N-CDs has emerged as a transformative strategy to overcome this limitation, significantly enhancing supercapacitor performance by synergistically improving specific capacitance, cycling stability, and charge–discharge efficiency.<sup>169–173</sup>

The enhancements provided by N-CDs are substantial and quantifiable, as detailed in Table 3. A prime example is the work by Li *et al.*<sup>174</sup> (Fig. 23), who demonstrated that incorporating nitrogen-doped graphene quantum dots (N-GQDs) into a cubic porous carbon matrix boosted the specific capacitance by approximately 65%, from a baseline of  $\sim 350 \text{ F g}^{-1}$  to  $\sim 580 \text{ F g}^{-1}$ . This performance leap is representative of a broader trend, with empirical studies consistently reporting N-CD-based composites achieving specific capacitances exceeding  $500 \text{ F g}^{-1}$  while maintaining exceptional cycling stability over 10 000 cycles.<sup>175–179</sup>

The incorporation of nitrogen dopants, particularly in the form of pyridinic-N and graphitic-N, introduces multifaceted advantages. Pyridinic-N atoms, located at the edges of the carbon lattice, donate lone-pair electrons to participate in reversible faradaic redox reactions, introducing significant pseudocapacitance that supplements the EDLC. Concurrently, graphitic-N, integrated within the carbon matrix, enhances the bulk electronic conductivity of the electrode by promoting  $\pi$ -electron delocalization, which facilitates faster electron transport and enables superior rate capability. Furthermore, the high surface area, abundant functional groups, and porous morphology of N-CD-based materials collectively improve electrolyte wettability and ion accessibility, thereby increasing the electrochemically active surface area and reducing ion diffusion resistance.<sup>161–163,180</sup>

N-CDs are incorporated into electrodes *via* various strategies, including direct deposition, composite formation with conductive polymers or two-dimensional materials, and hybridization with carbon nanotubes (CNTs). For instance, N-CD/graphene hybrids effectively prevent the restacking of graphene sheets, maximizing the surface area for ion adsorption while the N-CDs act as conductive bridges and pseudocapacitive



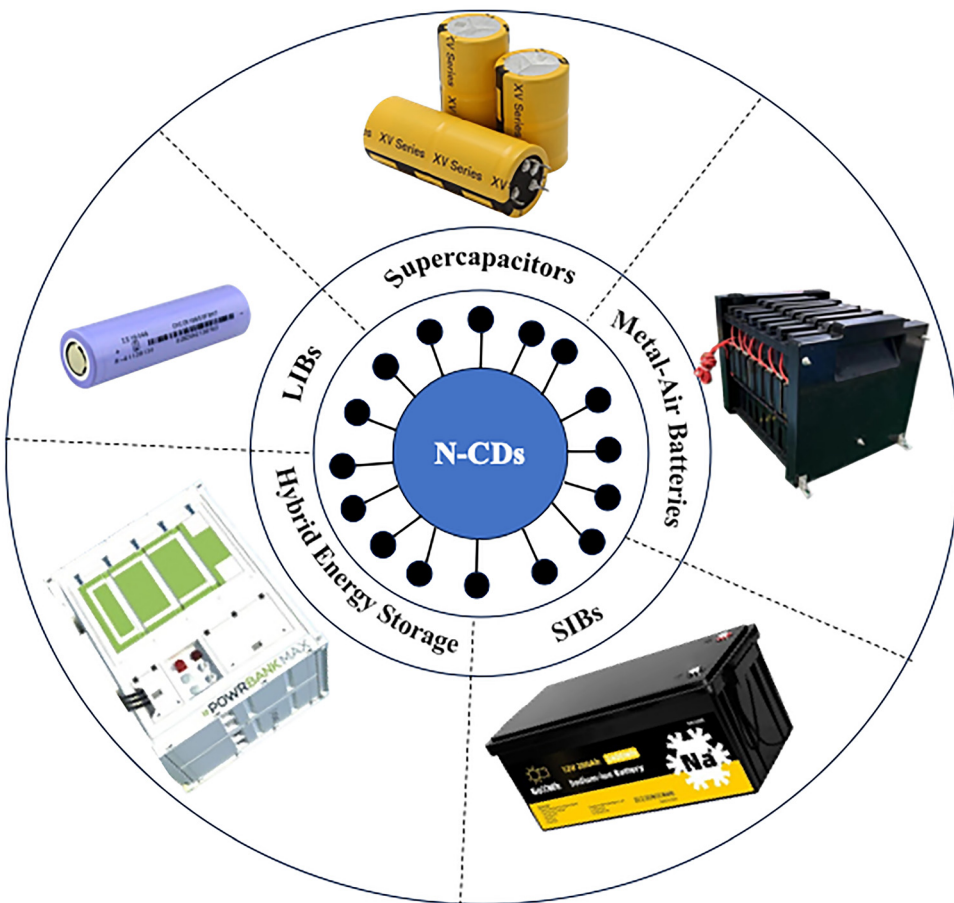


Fig. 22 Schematic overview of N-CDs applications in energy storage devices.

centers, leading to high energy density without compromising power or longevity.<sup>181–183</sup>

The collective evidence solidifies the role of N-CDs as powerful, multifunctional components in supercapacitors. They transcend the role of a simple additive by actively participating in the charge storage process through a threefold mechanism of action: introducing substantial pseudocapacitance *via* nitrogen functional groups, drastically improving electrode conductivity, and enhancing ion accessibility. This mechanistic synergy, as quantified in comparative studies, consistently translates to measurable and significant performance gains, firmly positioning N-CDs as key enablers for next-generation high-power, high-energy supercapacitors.

## 5.2 Lithium-ion batteries (LIBs)

LIBs serve as the cornerstone of modern energy storage, powering applications from portable electronics to electric vehicles. However, the pursuit of higher energy density, faster charging, and longer cycle life demands advanced electrode materials. The integration of nitrogen-doped carbon dots (N-CDs) into LIB architectures has emerged as a powerful strategy to address these challenges, demonstrating remarkable improvements in electrochemical performance, particularly in enhancing charge/discharge kinetics, rate capability, and long-term cycling stability.<sup>184–187</sup>

The performance enhancements afforded by N-CDs are significant and quantifiable. As systematically compared in Table 3, the modification of a conversion-type anode like  $\text{Fe}_3\text{O}_4$  with N-CDs can increase the specific capacity by  $\sim 37\%$ , from approximately  $800 \text{ mAh g}^{-1}$  to  $\sim 1100 \text{ mAh g}^{-1}$ , while simultaneously improving rate capability. This level of improvement is representative of a broader trend, with N-CD-modified anodes frequently achieving exceptional reversible capacities exceeding  $1000 \text{ mAh g}^{-1}$  at high current densities while maintaining outstanding cycling stability.<sup>149,150,164</sup>

These substantial gains are driven by specific micro- and mesoscopic mechanisms, a key focus of this review. When utilized as conductive additives or surface modifiers, N-CDs provide a multi-faceted improvement to electrode function. The highly conductive  $\text{sp}^2$  carbon network of N-CDs facilitates rapid electron transport to and from the active material, effectively reducing charge-transfer resistance.<sup>188–192</sup> Concurrently, the nitrogenous functional groups, particularly pyridinic-N and pyrrolic-N, play a critical role in electrochemistry at the electrode–electrolyte interface. These functional groups promote the formation of a more stable, robust, and ionically conductive solid-electrolyte interphase (SEI). A stable SEI is crucial as it minimizes irreversible lithium consumption during the initial cycles and suppresses detrimental side reactions during



Table 2 Multifunctional roles of N-CDs in energy storage devices

Energy storage system	Role of N-CDs	Mechanism/advantage	Performance impact	Ref.
Supercapacitors	Electrode material or additive to carbon-based electrodes.	Enhanced surface area, pseudo capacitance from N-sites, faster charge-discharge.	Higher specific capacitance, improved cycle stability.	144 145 146 147 148
Lithium-ion batteries	Anode modifier or conductive additive.	Improved electronic conductivity, better $\text{Li}^+$ intercalation, suppression of SEI growth.	Higher capacity retention, better rate performance.	149 150 151 152
Sodium-ion & potassium-ion batteries	Conductive matrix or coating material for anodes/cathodes.	Buffering volume changes, facilitated $\text{Na}^+/\text{K}^+$ ion diffusion, stable SEI formation.	Increased cycle life, higher initial coulombic efficiency.	153 154
Metal-air batteries (Zn-air, Li-air)	Cathode catalyst or electrolyte additive	Promotes $\text{O}_2$ reduction and evolution reactions; active nitrogen sites improve reaction kinetics.	Reduced overpotential, enhanced power density.	155 156 157
Hybrid energy storage systems	Component in electrode architecture	Dual-energy storage mechanics: synergy between battery-like and capacitor-like behavior.	Balanced energy and power density, extended life cycle.	158 159 160

Table 3 Quantitative performance enhancement of N-CD-based materials in energy storage devices

Device type	Electrode material	Key performance metric (control)	Key performance metric (with N-CDs)	Improvement (%)	Primary role/mechanism of N-CDs	Ref.
Supercapacitor	N-CD/graphene hybrid	Capacitance: $\sim 350 \text{ F g}^{-1}$	Capacitance: $\sim 580 \text{ F g}^{-1}$	+65%	Pseudocapacitance (pyridinic-N), enhanced conductivity (graphitic-N)	161 162
LIB	N-CD modified anode	Capacity: $\sim 800 \text{ mAh g}^{-1}$	Capacity: $\sim 1100 \text{ mAh g}^{-1}$	+37%	Conductive network, SEI stabilization	163 149 150 164
SIB	N-CD composite	Capacity retention (100 cycles): 70%	Capacity retention (100 cycles): 90%	+20%	Enhanced $\text{Na}^+$ adsorption, buffers volume change	165
Metal-air	N-CD catalyst	Discharge voltage: 1.25 V	Discharge voltage: 1.38 V	$\sim +10\% (\Delta V)$	ORR catalysis (pyridinic/graphitic-N)	166 167
Hybrid SC	$\text{Ni(OH)}_2/\text{N-CDs}$	Capacitance: $\sim 1200 \text{ F g}^{-1}$	Capacitance: $\sim 2100 \text{ F g}^{-1}$	+75%	Structural directing agent, conductive mediator	168

extended cycling, thereby enhancing the first-cycle coulombic efficiency and overall battery lifespan.<sup>118,193,194</sup>

The synthesis pathway itself can be tailored for dual functionality, as demonstrated by Wang *et al.*,<sup>195</sup> who developed a

sustainable approach for synthesizing both highly fluorescent N-CDs and bulk carbon anode materials from a single precursor (egg yolk) *via* a dual-phase hydrothermal method. This work underscores that the nitrogen doping responsible for the optical

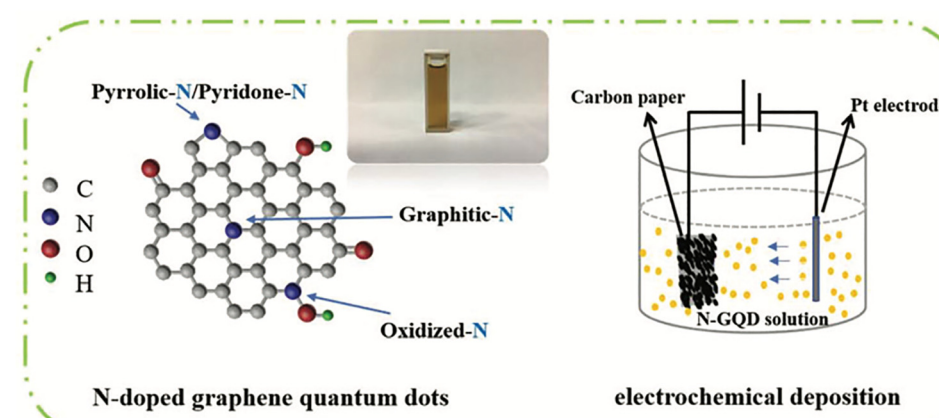


Fig. 23 Schematic illustration of N-GQDs and their electrochemical deposition process for supercapacitor applications.<sup>174</sup> Copyright 2018, Royal Society of Chemistry.



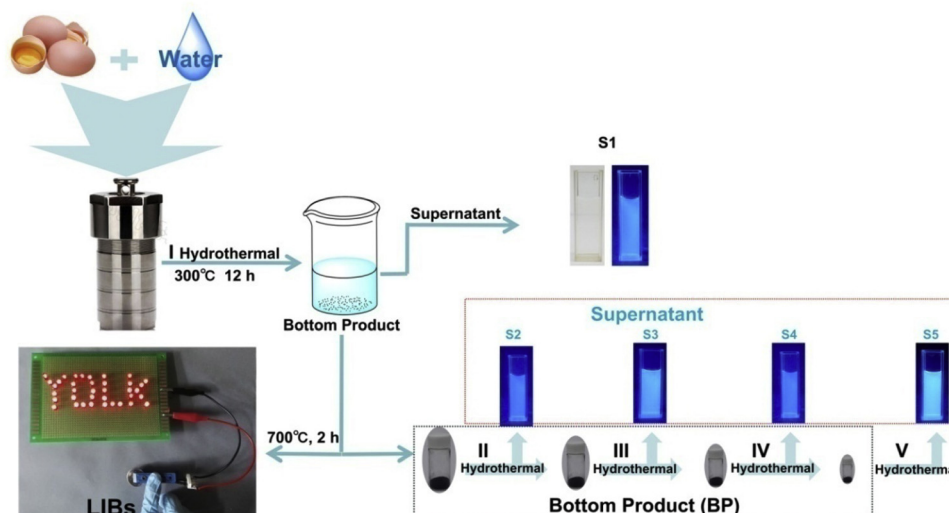


Fig. 24 Schematic illustration of the green hydrothermal synthesis process for N-CDs and derived bulk carbon anode materials for LIB applications.<sup>195</sup> Copyright 2018, Elsevier.

properties of the N-CDs also improves electrical conductivity and creates additional active sites for  $\text{Li}^+$  storage in the resulting bulk carbon, which exhibited exceptional anode performance. This highlights the promise of biomass-derived, N-CD-enhanced materials for sustainable LIB development (Fig. 24).

In summary, the integration of N-CDs addresses several fundamental limitations in LIBs. They act as more than simple conductive agents; they are multifunctional modifiers that enhance bulk conductivity, guide the formation of a superior SEI layer, and provide additional active sites for lithium storage. This mechanistic synergy, evidenced by clear quantitative improvements in capacity and stability, positions N-CDs as transformative components for advancing next-generation, high-performance lithium-ion battery technologies.

### 5.3 Sodium-ion batteries (SIBs) and potassium-ion batteries (PIBs)

Sodium-ion (SIBs) and potassium-ion batteries (PIBs) have emerged as promising, cost-effective alternatives to lithium-ion systems for large-scale grid storage, owing to the natural abundance of sodium and potassium. However, their development is hampered by fundamental challenges arising from the larger ionic radii of  $\text{Na}^+$  and  $\text{K}^+$ , which lead to sluggish ion diffusion kinetics and severe electrode structural instability during cycling. The integration of nitrogen-doped carbon dots (N-CDs) effectively addresses these challenges by enhancing bulk conductivity, stabilizing electrode architectures, and facilitating rapid ion transport, thereby positioning N-CDs as key enablers for these post-lithium technologies.<sup>196–200</sup>

The efficacy of N-CDs in mitigating these issues is demonstrated by clear, quantitative performance gains. As highlighted in Table 3, the incorporation of N-CDs into carbon anodes for SIBs can improve capacity retention after 100 cycles from 70% to 90%, representing a significant 20% enhancement in cycling stability. This level of improvement is characteristic, with studies frequently reporting N-CD-modified SIB anodes achieving high reversible capacities exceeding  $400 \text{ mAh g}^{-1}$  while

maintaining exceptional rate capability and stability over 1000+ cycles.<sup>199,201–204</sup>

The multifunctionality of N-CDs extends beyond the electrode itself. Lee *et al.*,<sup>205</sup> demonstrated their innovative use as electrolyte additives in sodium metal batteries. Their work revealed that N-CDs modify the  $\text{Na}^+$  solvation structure, leading to more uniform  $\text{Na}$  plating/stripping, a more stable solid electrolyte interphase (SEI), and dramatically improved cycling stability and coulombic efficiency (Fig. 25). This establishes N-CDs as a novel class of electrolyte modifiers that tackle interfacial instability, a fundamental challenge in metal anode systems.

Furthermore, N-CDs can be architecturally integrated to create synergistic composites. This is exemplified by the work of Li *et al.*,<sup>206</sup> who developed a PIB anode by anchoring FeSb nanoparticles within a 3D porous nitrogen-doped carbon matrix, with N-CDs directly on the FeSb surfaces. In this hierarchical design, the N-CDs performed three critical functions: creating conductive electron pathways, providing additional active sites for  $\text{K}^+$  storage, and enabling pseudocapacitive charge storage. This synergy resulted in a high reversible capacity of  $\sim 245 \text{ mAh g}^{-1}$  at a very high current density of  $3080 \text{ mA g}^{-1}$  after 1000 cycles, showcasing exceptional rate capability and stability (Fig. 26).

The engineered surface chemistry of N-CDs plays a pivotal role. Oxygen- and nitrogen-containing functional groups enhance the electrode's affinity for  $\text{Na}^+/\text{K}^+$  ions, improving initial coulombic efficiency and adsorption kinetics. Simultaneously, the robust  $\text{sp}^2$  carbon structure of N-CDs acts as a conductive buffer, mitigating the substantial volume changes of alloying or conversion-type anodes (*e.g.*, FeSb) during repeated ion insertion/extraction, thus preventing mechanical pulverization and ensuring long-term durability.<sup>165</sup>

In conclusion, N-CDs serve as versatile components that directly address the core limitations of SIBs and PIBs. Their unique properties, tunable surface chemistry for enhanced ion affinity, a robust structure for mechanical buffering, and high conductivity for efficient charge transport work in concert to



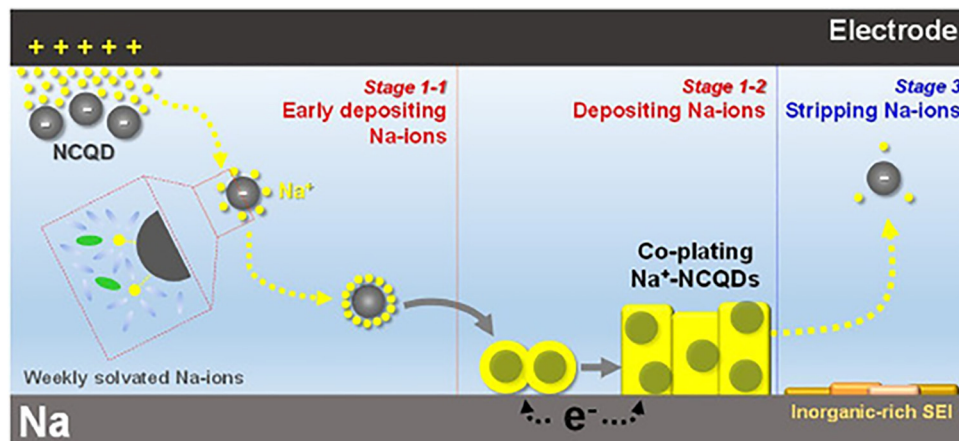


Fig. 25 Mechanism of N-CDs in regulating  $\text{Na}^+$  deposition/stripping behavior and stabilizing the SEI in SIBs.<sup>205</sup> Copyright 2025, Elsevier.

improve cycling stability, capacity, and rate performance. The advanced applications as both electrode modifiers and electrolyte additives underscore their transformative potential in guiding the development of practical and durable next-generation alkali-ion battery systems.

#### 5.4 Metal-air batteries (Zn-air, Li-air)

Metal-air batteries, particularly lithium-air (Li-air) and zinc-air (Zn-air) systems, are leading candidates for next-generation energy storage due to their exceptional theoretical energy densities.<sup>207–209</sup> However, their practical application is hindered by the sluggish kinetics of the oxygen reduction (ORR) and evolution (OER) reactions at the cathode. Nitrogen-doped carbon dots (N-CDs) have emerged as highly efficient, metal-free electrocatalysts that directly address this bottleneck, offering a compelling alternative to expensive and scarce noble-metal catalysts like Pt and  $\text{RuO}_2$ .<sup>210–212</sup>

The catalytic prowess of N-CDs translates into direct and quantifiable performance gains. As systematically compared in Table 3, a cathode based on N-CDs can increase the discharge voltage of a Zn-air battery from 1.25 V to 1.38 V,<sup>166,167</sup> a significant reduction in overpotential that directly boosts the system's efficiency and energy output. This level of

improvement is a hallmark of N-CD integration, with studies consistently reporting enhanced power density and extended cycle life compared to unmodified carbon-based cathodes.<sup>212–214</sup>

This superior electrocatalytic performance, observable across various system configurations (aqueous, aprotic, hybrid, and solid-state), is rooted in the unique physicochemical properties of N-CDs. The catalytic activity is primarily driven by specific nitrogen configurations. Pyridinic-N sites, with their lone-pair electrons, optimize the adsorption of oxygen intermediates, while graphitic-N species enhance the electron transfer capability of the carbon matrix. This synergistic action significantly accelerates ORR/OER kinetics. Furthermore, the inherently high surface area, tunable porosity, and abundant edge sites of N-CDs create an ideal architecture that maximizes the exposure of active sites and facilitates efficient mass transport of both oxygen and electrolyte, thereby improving overall catalytic efficiency and durability.<sup>213,215–217</sup>

A seminal study by Lin *et al.*,<sup>218</sup> powerfully demonstrates the transformative role of N-CDs in complex architectures. They developed a breakthrough lithium–oxygen battery cathode by constructing a hierarchical  $\text{FePc}/\text{N-CD}/\text{Co}_3\text{O}_4$  hybrid. In this design, the N-CDs served dual critical functions: acting as conductive bridges between catalytic phases and serving as catalytically active centers themselves. Their ultrasmall size ( $<5$  nm) enabled atomic-level dispersion, which, combined with their ability to stabilize the Fe–N coordination environment, led to exceptional bifunctional activity. The resulting composite achieved a remarkable specific capacity of  $28619 \text{ mAh g}^{-1}$  at  $200 \text{ mA g}^{-1}$  and maintained stable operation for over 350 cycles, a substantial advancement attributable to N-CD-mediated enhancements in both electronic conductivity and catalytic durability (Fig. 27).

In summary, N-CDs have proven to be indispensable components for advancing metal-air battery technology. They function as multifunctional electrocatalysts whose activity is precisely tuned by their nitrogen configuration. By providing efficient, stable, and cost-effective catalytic sites, facilitating charge transfer, and enhancing mass transport, N-CDs directly

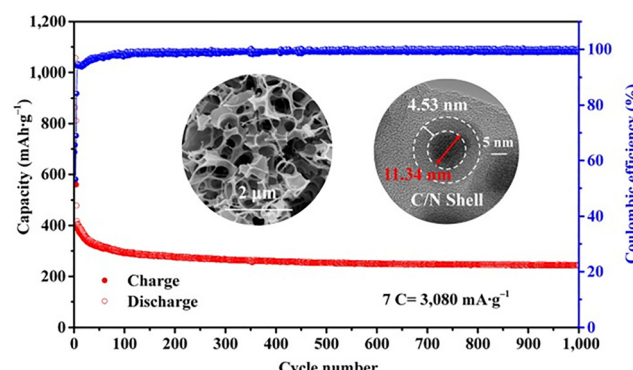


Fig. 26 Long-term cycling stability and structural integrity of the N-CQD-enhanced FeSb composite anode in PIBs.<sup>206</sup> Copyright 2022, Springer.



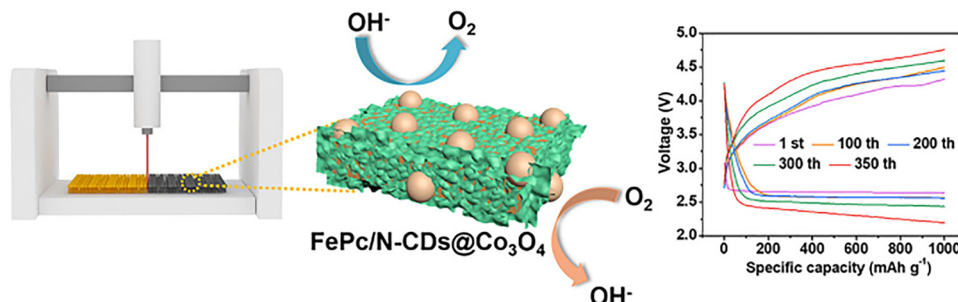


Fig. 27 Schematic illustration and electrochemical performance of FePc/N-CDs@Co<sub>3</sub>O<sub>4</sub> cathode for lithium–oxygen batteries.<sup>218</sup> Copyright 2022, Springer.

address the key limitations that have hindered the commercialization of these high-energy-density systems, positioning them as a cornerstone material for future development.

### 5.5 Hybrid energy storage systems

Hybrid energy storage systems are engineered to bridge the performance gap between the high energy density of batteries and the high power density of supercapacitors, meeting the growing demand for versatile power solutions in applications ranging from electric vehicles to grid storage and flexible electronics.<sup>202,219,220</sup> Nitrogen-doped carbon dots (N-CDs) are uniquely suited for these systems due to their intrinsic ability to contribute to both capacitive (electric double-layer) and faradaic (pseudocapacitive/battery-like) charge storage mechanisms. This dual functionality, enabled by their high surface area, nitrogen redox-active sites, and conductive sp<sup>2</sup> carbon networks, allows N-CDs to enhance charge storage capacity, improve cycling stability, and accelerate ion transport, effectively balancing energy and power characteristics in a single device.<sup>221,222</sup>

The impact of N-CD integration is profound and quantifiable. As a prime example highlighted in Table 3, the incorporation of N-CDs into a nickel hydroxide (Ni(OH)<sub>2</sub>) electrode resulted in a dramatic 75% increase in specific capacitance, from a baseline of ~1200 F g<sup>-1</sup> to an enhanced value of ~2100 F g<sup>-1</sup>.<sup>168</sup> This substantial improvement underscores the ability of N-CDs to unlock synergistic performance in hybrid architectures.<sup>221,223</sup>

The mechanisms behind this synergy are multifaceted and operate at the micro- and mesoscopic scales. In such composites, N-CDs perform several critical roles simultaneously. They act as conductive mediators, creating electron superhighways that drastically improve charge transfer within the often less-conductive battery-type material (e.g., Ni(OH)<sub>2</sub>).<sup>224</sup> Concurrently, their own nitrogen functional groups (particularly pyridinic-N) contribute significant pseudocapacitance through reversible redox reactions. Furthermore, as demonstrated by Yuksel *et al.*<sup>225</sup> N-CDs can serve as structural directors that control the nucleation and growth of active materials. In their work on a Ni(OH)<sub>2</sub>/N-CD composite, the N-CDs promoted the formation of ultrathin, well-dispersed Ni(OH)<sub>2</sub> nanosheets, preventing aggregation and yielding a more uniform, highly porous architecture that maximizes the exposed electroactive

surface area and facilitates enhanced ion diffusion (Fig. 28). This structural control, combined with improved conductivity and additional pseudocapacitance, results in electrodes that achieve an exceptional combination of high energy density, excellent rate capability, and long-term cycling stability.

In conclusion, N-CDs are far more than simple additives in hybrid systems; they are multifunctional integrators that fundamentally enhance electrode architecture and kinetics. By providing conductive pathways, intrinsic charge storage, and nanoscale structural control, they effectively unify the high-energy and high-power attributes of different charge storage mechanisms. This ability to engineer synergistic composites positions N-CDs as a cornerstone material for the development of next-generation hybrid energy storage devices capable of meeting the complex demands of modern technology.

## 6 Recent advances in N-CDs/polymer and N-CDs/metal nanocomposites for energy storage

Polymers and nanocomposites play a pivotal role in advancing the performance and versatility of modern energy storage devices. Conductive polymers such as polyaniline (PANI), poly-pyrrole (PPy), and poly(3,4-ethylenedioxythiophene) (PEDOT) are widely studied due to their intrinsic electrical conductivity,

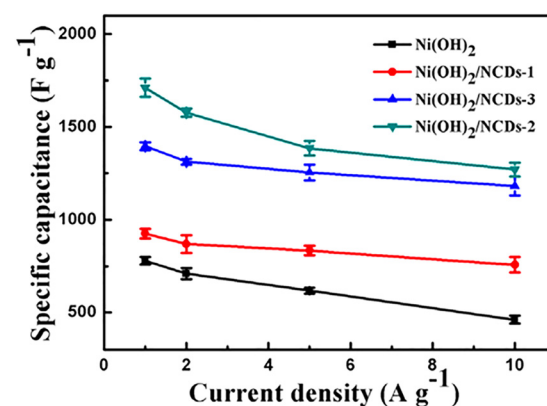


Fig. 28 Electrochemical performance of Ni(OH)<sub>2</sub>/N-CDs composite electrodes in hybrid supercapacitor applications.<sup>225</sup> Copyright 2019, Elsevier.



mechanical flexibility, and pseudocapacitive behavior.<sup>226–228</sup> Their rapid redox reactions make them particularly suitable for high-rate charge–discharge applications in supercapacitors and batteries. When combined with materials like metal oxides (*e.g.*, ZnO), carbon nanotubes, graphene, or metal-organic frameworks (MOFs), these polymers form nanocomposites with enhanced electrochemical properties.<sup>229,230</sup>

Recently, incorporating N-CDs into polymeric and metallic nanocomposites has emerged as a promising strategy for improving the performance of supercapacitors, batteries, and hybrid energy systems.<sup>231–233</sup> This section highlights recent advances in N-CD-based nanocomposites, focusing on their role in energy storage, electrode enhancement, and solid-state electrolytes for next-generation batteries.

### 6.1 N-CDs/conductive polymer hybrids for flexible energy storage

The growing demand for flexible and wearable energy storage devices has driven extensive research into conductive polymers, including polyaniline (PANI), polypyrrole (PPy), and poly(3,4-ethylenedioxythiophene) (PEDOT). These polymers are particularly attractive due to their intrinsic conductivity, mechanical flexibility, and reversible redox activity, making them ideal for supercapacitors and batteries. Recent studies demonstrate that incorporating nitrogen-doped carbon dots (N-CDs) into these

polymers significantly enhances their electrochemical performance, yielding higher specific capacitance, improved cycling stability, and superior mechanical durability.<sup>234–236</sup>

The synergy between N-CDs and conductive polymers enhances charge storage through multiple mechanisms. N-CDs introduce additional redox-active sites, boosting faradaic activity, while their high electrical conductivity facilitates efficient electron transport. Moreover, the functional groups on N-CDs strengthen polymer–electrolyte interactions, optimizing ion diffusion. Specific nitrogen configurations, such as pyridinic-N and pyrrolic-N, enhance pseudocapacitive behavior, whereas graphitic-N improves electronic conductivity. These functional groups also promote uniform polymer dispersion and reinforce the composite's structural integrity.<sup>237–242</sup>

Xie *et al.*<sup>243</sup> developed morphology-tunable nitrogen-doped carbon dots/polyaniline (N-CDs@PANI) hybrids to systematically evaluate their electrochemical performance for supercapacitor applications. Their work revealed that N-CDs integration significantly enhances PANI's conductivity, surface area, and pseudocapacitive properties. Crucially, the study established a morphology–performance relationship, demonstrating that optimized hybrid nanostructures exhibit superior capacitance, making them promising candidates for high-performance flexible supercapacitor electrodes (Fig. 29).

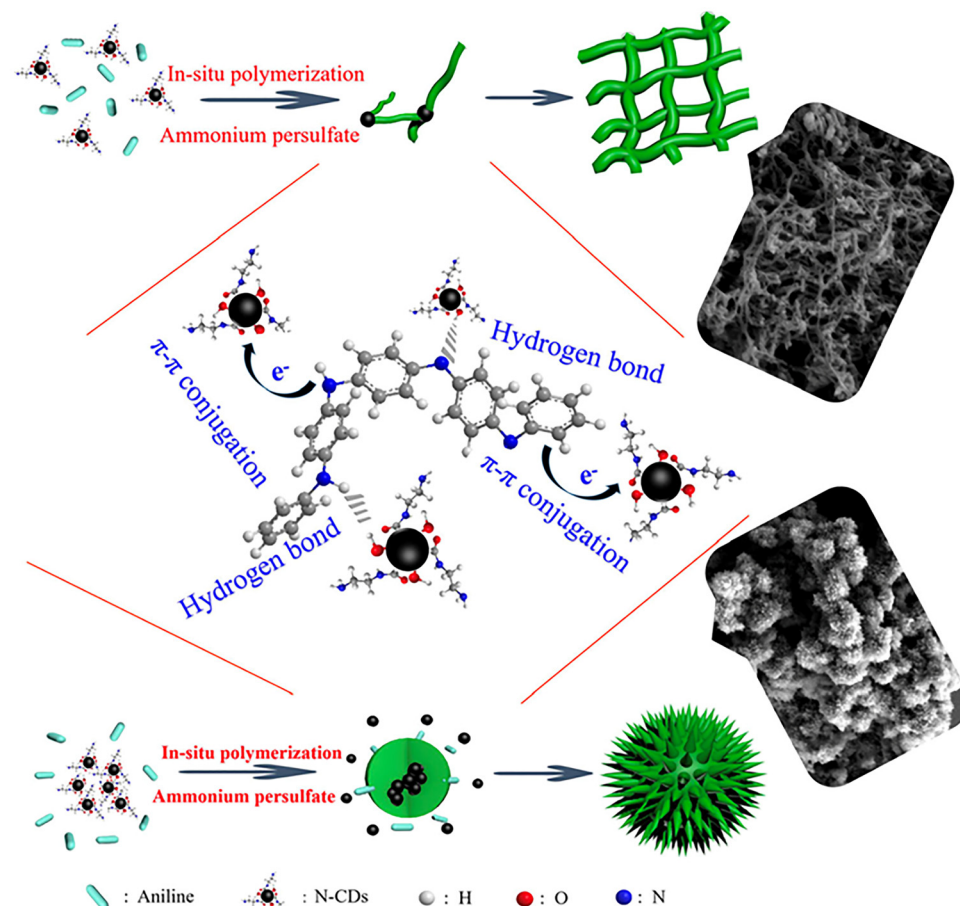


Fig. 29 Schematic illustration of the *in situ* oxidative polymerization process for N-CDs@PANI hybrid fabrication.<sup>243</sup> Copyright 2014, Wiley.



In conclusion, the integration of N-CDs into conductive polymers creates a synergistic relationship that addresses the typical limitations of both materials. The literature shows that N-CDs mitigate the cycling instability of polymers by providing a robust conductive scaffold, while the polymers offer a high-capacity matrix that leverages the surface functionality of the dots. This strategy is particularly effective for developing high-performance, flexible energy storage devices.

## 6.2 N-CDs/metal oxide and sulfide nanocomposites for enhanced electrochemical performance

Metal oxides and sulfides have emerged as prime candidates for energy storage electrodes due to their high theoretical capacity and rich redox activity. However, their practical implementation faces fundamental challenges, including poor electrical conductivity, sluggish ion diffusion kinetics, and structural instability during repeated charge–discharge cycles. Recent advances have demonstrated that N-CDs serve as multifunctional modifiers that effectively overcome these limitations. The incorporation of N-CDs into metal oxide/sulfide matrices significantly enhances charge transfer kinetics while simultaneously improving cycling stability through structural reinforcement.<sup>244–247</sup>

Substantial improvements in electrochemical performance have been achieved through the integration of N-CDs with metal oxides like ZnO, TiO<sub>2</sub>, MnO<sub>2</sub>, and Fe<sub>2</sub>O<sub>3</sub>. The synergistic interaction between N-CDs and metal oxides manifests in three primary ways: enhanced electron transport through conductive pathways created by N-CDs, suppressed charge recombination due to interfacial charge trapping at N-CD sites, and increased electroactive surface area resulting from nanostructural modulation. These combined effects lead to substantial improvements in specific capacitance and energy density compared to unmodified metal oxide electrodes.<sup>248–252</sup>

Li *et al.*<sup>253</sup> developed photoresponsive supercapacitor electrodes by decorating zinc oxide (ZnO) with N-CDs. The N-CDs modification substantially enhanced the electrochemical performance of ZnO electrodes, demonstrating a remarkable 58.9% improvement in areal capacitance under UV illumination compared to dark conditions. The optimized ZnO/N-CDs composite achieved a maximum areal capacitance of 2.6 mF cm<sup>-2</sup> at 1.6  $\mu$ A cm<sup>-2</sup> current density following photocharging and galvanostatic discharge cycles (Fig. 30), highlighting its potential for light-assisted energy storage applications.

Similarly, layered transition metal sulfides, particularly MoS<sub>2</sub>, NiS, and SnS<sub>2</sub>, have garnered considerable research interest owing to their unique structural characteristics and intrinsic electrocatalytic properties. Despite these advantages, their widespread deployment in energy storage systems has been constrained by two fundamental limitations: insufficient electrical conductivity and progressive structural degradation during repeated charge–discharge cycles. Recent advances have demonstrated that N-CDs serve as multifunctional additives that effectively address these challenges through simultaneous enhancement of charge transport properties, structural stabilization, and improved electrolyte accessibility.<sup>246,254</sup>

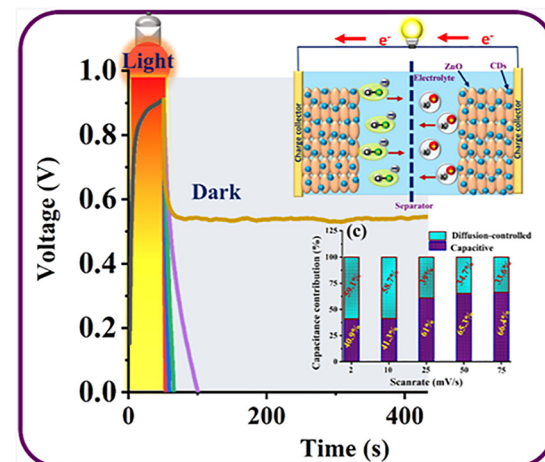


Fig. 30 Electrochemical performance characterization of the ZnO/N-CD composite supercapacitor electrode.<sup>253</sup> Copyright 2023, American Chemical Society.

Notable progress has been achieved through several innovative material designs. Cui *et al.*<sup>255</sup> developed a high-performance hybrid supercapacitor system based on cobalt sulfide/reduced graphene oxide composites modified with N-CDs. The incorporation of N-CDs enhanced the electrical conductivity, surface area, and electrochemical activity of the composite material. The resulting CoS/N-doped CDs/rGO/N-doped CDs electrode exhibited excellent specific capacitance, superior energy density, and outstanding cycling stability (Fig. 31).

In a complementary approach focusing on sustainable materials, Yu *et al.*<sup>256</sup> developed a high-performance anode material for hybrid supercapacitors by anchoring lignin-derived nitrogen-doped carbon dots (N-CDs) onto a NiCo<sub>2</sub>S<sub>4</sub>/graphene hydrogel composite. The integration of sustainable N-CDs significantly improved electron conductivity, surface area, and redox activity, enabling the hybrid electrode to exhibit high specific capacity, excellent rate capability, and long cycling stability (Fig. 32).

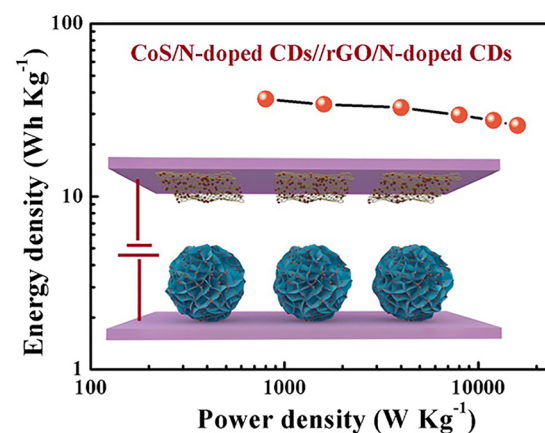


Fig. 31 Schematic illustration of the CoS/N-CDs/rGO hybrid supercapacitor electrode showing synergistic enhancement mechanisms.<sup>255</sup> Copyright 2020, Elsevier.



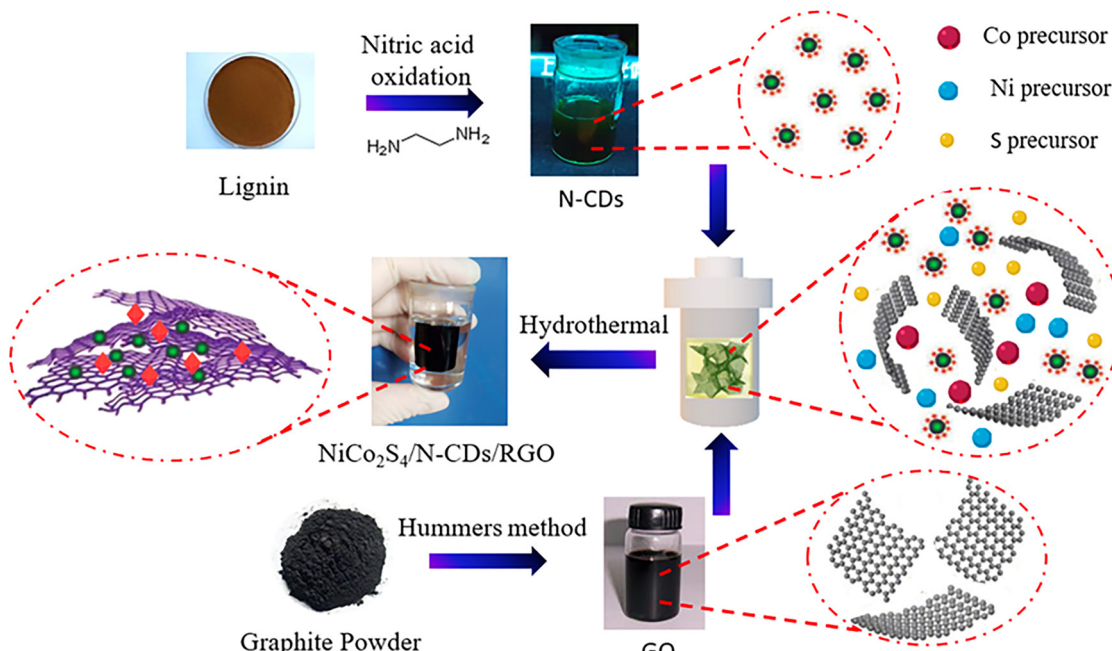


Fig. 32 Fabrication schematic of the  $\text{NiCo}_2\text{S}_4/\text{N-CDs/RGO}$  ternary hydrogel composite.<sup>256</sup> Copyright 2017, MDPI.

The superior electrochemical performance of N-CD/metal oxide and sulfide composites can be attributed to three key factors: (1) the high electrical conductivity imparted by N-CDs, (2) reduced charge transfer resistance at the electrode–electrolyte interface, and (3) the prevention of particle aggregation and structural collapse. Furthermore, the porous architecture of N-CDs promotes rapid ion diffusion and provides additional active sites for charge storage, further boosting the overall performance of these nanocomposites.<sup>257–259</sup>

### 6.3 The impact of N-CDs in solid-state electrolytes for next-generation batteries

Solid-state batteries (SSBs) have emerged as a transformative energy storage technology, offering superior safety and energy density compared to conventional liquid electrolyte systems. Their non-flammable nature and enhanced thermal stability address critical safety concerns, yet significant challenges persist in achieving commercially viable performance. Two fundamental limitations, suboptimal ionic conductivity and unstable electrode–electrolyte interfaces, have remained key barriers to widespread adoption. Recent breakthroughs demonstrate that nitrogen-doped carbon dots (N-CDs) serve as multifunctional additives capable of addressing these challenges through unique physicochemical mechanisms.<sup>260,261</sup>

The exceptional performance enhancement provided by N-CDs stems from their distinctive structural and chemical properties. Surface characterization studies reveal that the abundant oxygen- and nitrogen-containing functional groups on N-CDs (including carboxyl, hydroxyl, and various nitrogen configurations) create favorable binding sites for lithium ions. This interaction significantly improves ionic conductivity, with experimental measurements showing increases of 2–3 orders of

magnitude in N-CD-modified polymer electrolytes compared to unmodified counterparts. Moreover, the nanoscale dimensions of N-CDs (typically 2–10 nm) enable the formation of continuous ion transport networks that simultaneously reduce interfacial impedance while enhancing overall cell stability.<sup>262</sup>

A particularly critical challenge in solid-state battery development involves establishing and maintaining stable interfaces between the electrolyte and electrodes. N-CDs address this challenge through several mechanisms. Their incorporation into solid-state electrolytes improves interfacial contact by reducing surface roughness and optimizing ion diffusion kinetics. Additionally, N-CD-enhanced polymer electrolytes demonstrate superior mechanical strength and flexibility compared to conventional materials, properties that are crucial for preventing electrolyte degradation during repeated charge–discharge cycles.<sup>263,264</sup>

Li *et al.*<sup>265</sup> fabricated an all-solid-state flexible supercapacitor by integrating nitrogen- and oxygen-co-doped graphene quantum dots (N/O-QGDs), a specific form of nitrogen-doped carbon dots (N-CDs), onto a 3D carbon nanotube/carbon cloth (CNT/CC) framework. The N-CDs played a critical role in enhancing the device's electrochemical performance by providing abundant nitrogen-related active sites that facilitate faradaic redox reactions, thus contributing significantly to pseudocapacitance. Additionally, the quantum confinement and heteroatom doping endowed the N-CDs with high electrical conductivity and improved charge carrier density, which accelerated electron transfer kinetics at the electrode interface (Fig. 33).

## 7 Challenges and future perspectives

Although N-CDs have shown significant promise in energy storage applications, several challenges must be overcome



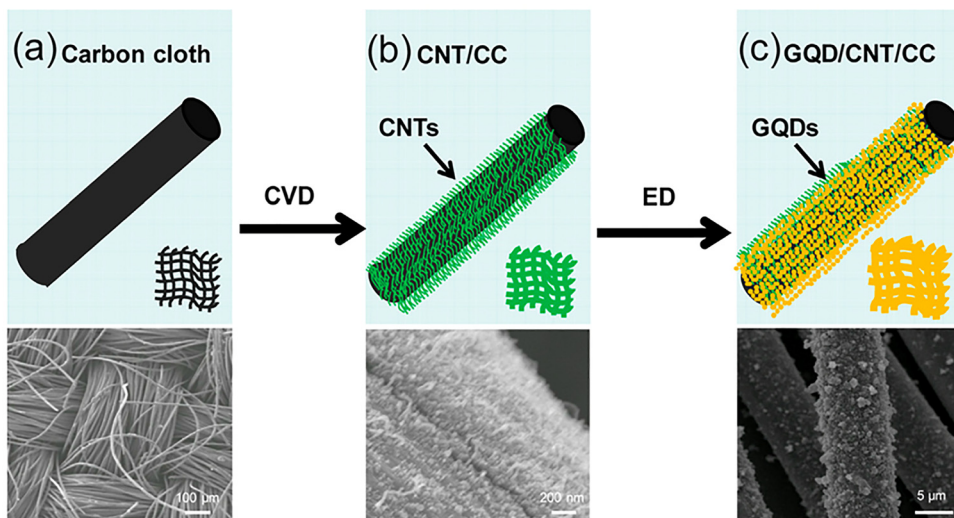


**Fig. 33** Schematic illustration for the preparation of 3D N-O-GQD/CNT/CC electrodes. (a) Pristine carbon cloth (CC) substrate. (b) CNTs grown on CC via CVD to form CNT/CC composite. (c) N-O-GQDs electrodeposited on CNT/CC to yield the final 3D N-O-GQD/CNT/CC electrode. Bottom panels show corresponding SEM images at different magnifications.<sup>265</sup> Copyright 2017, Elsevier.

before they can reach their full potential. Issues such as scalability, stability, electrochemical performance, and commercial viability remain barriers to widespread adoption. Addressing these challenges will require innovative synthesis methods, performance enhancements, and better integration into next-generation energy storage systems. This section discusses the key challenges facing N-CDs in energy storage and explores future research directions and emerging trends that could enable their practical implementation.

### 7.1 Scalability and cost-effective production of N-CDs

A major obstacle to the widespread adoption of N-CDs in energy storage is the scalability of their synthesis. While high-performance materials have been achieved at the laboratory scale, transitioning these methods to industrial-scale production remains challenging.<sup>202</sup>

Current synthesis techniques, such as hydrothermal, microwave-assisted, and electrochemical methods, require precise control over reaction conditions, precursor selection, and purification steps. Maintaining consistent particle size, nitrogen content, and functional groups becomes increasingly difficult at larger scales. For instance, hydrothermal synthesis operates under high temperatures, complicating large-scale production.<sup>266</sup>

Additionally, the reliance on expensive precursors and energy-intensive processes raises economic concerns. Transitioning to biomass-derived or waste-based carbon sources could offer a more sustainable and cost-effective approach. Furthermore, adopting green synthesis techniques, minimizing hazardous chemicals, and reducing energy consumption will be critical for industrial scalability.<sup>267</sup>

### 7.2 Techno-economic analysis and application outlook

The commercial translation of N-CDs depends critically on their techno-economic viability, which is governed by precursor costs, energy consumption, and purification processes.

Synthesis routes utilizing waste biomass, such as prickly pear or palm kernel shells, present a compelling economic advantage by minimizing precursor expenses and supporting a circular economy.<sup>23</sup> In contrast, methods relying on refined chemical precursors or energy-intensive techniques like chemical vapor deposition face significant economic hurdles for large-scale implementation, where cost-per-kilogram is a decisive factor, despite their ability to yield high-performance materials.<sup>22</sup>

The application landscape for N-CDs can be stratified by performance-to-cost ratio. Short-term opportunities reside in high-value, performance-critical domains where their functional benefits justify a premium. This includes their use as conductive additives in next-generation lithium-ion batteries for premium electric vehicles and as non-precious metal electrocatalysts in metal-air batteries.<sup>17</sup> For long-term, large-scale impact, the focus must shift to overcoming scalability challenges to achieve cost parity with conventional carbons. The most promising mass markets are stationary grid storage, where the exceptional cycling stability of N-CD-enhanced supercapacitors and sodium/potassium-ion batteries can reduce the levelized cost of storage, and low-cost, flexible electronics, leveraging the solution processability of N-CDs for printed and wearable devices. Realizing this potential will require concerted efforts in continuous flow synthesis, reactor design, and comprehensive life-cycle assessments, supported by strategic academia-industry partnerships to pilot and validate these technologies.<sup>136</sup>

### 7.3 Stability and long-term performance in energy storage devices

For N-CDs to be viable in energy storage applications, long-term stability and durability across numerous charge/discharge cycles are critical. However, several factors can degrade their performance over time.<sup>267</sup>



N-CDs are susceptible to surface oxidation, agglomeration, and functional group loss during prolonged cycling, which can reduce charge storage capacity and energy efficiency. To mitigate these issues, strategies such as surface passivation or protective functionalization could be explored. For example, coating N-CDs with conductive polymers or carbon shells may improve their stability under harsh electrochemical conditions.<sup>244,258</sup>

Additionally, the interaction between N-CDs and electrolytes, particularly under extreme conditions (e.g., high voltage, elevated temperatures), can significantly impact electrochemical performance. Further research is needed to evaluate N-CD/electrolyte compatibility, along with the development of hybrid electrolytes tailored for N-CD-based systems. For instance, ionic liquid-based electrolytes could enhance N-CD stability in high-voltage applications.<sup>268</sup>

#### 7.4 Strategies for enhancing electrochemical performance and cyclability

The nitrogen doping level and types of nitrogen-containing functional groups critically influence charge storage behavior. By precisely controlling these factors during synthesis, conductivity, redox activity, and ion diffusion can be significantly enhanced. For example, optimizing the pyridinic-N to graphitic-N ratio can improve both pseudocapacitive and conductive properties.<sup>269</sup>

Integrating N-CDs with advanced nanostructures, such as core-shell designs or porous networks, could further enhance charge transfer kinetics and electrochemically active surface area. Promising results have already been demonstrated in N-CD-based composites with materials like metal oxides, sulfides, or conductive polymers, warranting further exploration. For instance, N-CD/MoS<sub>2</sub> composites have shown improved lithium-ion storage capacity and cycling stability.<sup>235</sup>

A major challenge in energy storage is balancing high energy density (crucial for batteries) with high power density (essential for supercapacitors). Hybrid systems combining N-CD-based

electrodes with complementary materials could resolve this trade-off. For example, N-CD/graphene hybrids exhibit both high energy and power densities, making them ideal for hybrid supercapacitor-battery applications.<sup>223</sup>

#### 7.5 Potential for integration into commercial energy storage systems

For widespread adoption, N-CDs must be compatible with established electrode fabrication methods such as slurry coating and inkjet printing. Alternative approaches like binder-free electrode designs and direct deposition techniques could facilitate scalable production. Advanced manufacturing methods, including electrospinning and 3D printing, may enable precise fabrication of N-CD-based electrodes with controlled morphology and architecture.<sup>270</sup>

Beyond conventional batteries and supercapacitors, N-CDs show significant promise for next-generation energy storage applications, including metal-air batteries, flexible/wearable devices, and solid-state batteries. Their lightweight nature, tunable surface chemistry, and high electroactivity make them particularly suitable for these emerging technologies. For instance, N-CD-modified solid-state electrolytes have demonstrated improved ionic conductivity and interfacial stability in all-solid-state battery configurations.<sup>270</sup>

The commercialization of N-CD-based technologies requires careful consideration of environmental impacts throughout their lifecycle. Comprehensive life cycle assessments (LCAs) will be essential to evaluate the sustainability of large-scale production and disposal processes. Concurrently, developing greener synthesis methods and ensuring regulatory compliance will be critical for successful market adoption.<sup>271</sup>

#### 7.6 Future directions in research and emerging trends

##### 7.6.1 Machine learning and AI-driven material discovery.

The integration of artificial intelligence (AI) and machine

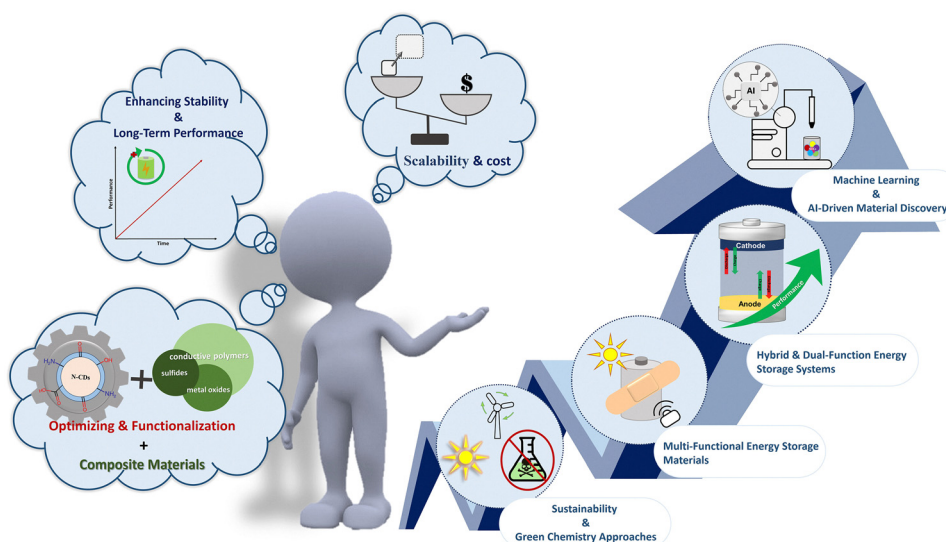


Fig. 34 Research roadmap for optimizing N-CD performance in energy storage applications, highlighting key focus areas: (1) advanced synthesis methods, (2) mechanistic understanding, (3) hybrid material integration, and (4) real-world device testing.



learning in materials science could revolutionize the discovery of optimal N-CD configurations. These computational approaches may enable predictive modeling of doping strategies, surface modifications, and composite architectures. For example, combining high-throughput screening with AI algorithms (Fig. 34) could accelerate the development of N-CDs with precisely tailored electrochemical properties.

**7.6.2 Multi-functional energy storage materials.** Future research should explore N-CD materials that combine energy storage with additional functionalities such as self-healing, photocatalytic activity, or sensing capabilities. These advanced materials could enable next-generation smart energy devices – for instance, self-repairing N-CD electrodes that automatically restore their electrochemical performance after physical damage, thereby significantly extending device lifetimes.

**7.6.3 Hybrid energy storage architectures.** N-CDs show particular promise for innovative hybrid energy storage systems, including supercapacitor-battery combinations and dual-ion battery configurations. Their unique properties could help overcome current performance limitations, for example, N-CD-enhanced dual-ion batteries capable of simultaneous cation and anion storage may achieve substantially higher energy densities than conventional systems.

**7.6.4 Sustainable development pathways.** Adopting green chemistry principles in N-CD research is crucial for sustainable energy storage solutions. This includes utilizing biomass-derived precursors, optimizing synthetic processes for minimal environmental impact, and developing biodegradable components. Bio-sourced N-CDs represent a particularly promising direction, offering both ecological and economic advantages over conventional materials.

## 8 Conclusion

This review has provided a comprehensive analysis of nitrogen-doped carbon dots (N-CDs) for electrochemical energy storage, establishing a critical link between synthesis parameters, nitrogen configurations, and electrochemical performance across supercapacitors, metal-ion batteries, and metal-air systems. A key distinction of this work is its integration of a first-of-its-kind techno-economic and application roadmap with fundamental material science, offering a practical guide for the rational design of next-generation N-CD-based materials.

Despite the significant progress documented herein, the path to commercialization requires overcoming persistent challenges in scalable, low-cost production, long-term cycling stability, and seamless integration into full-cell devices. Future research must prioritize the precise control of nitrogen doping configurations to fine-tune charge storage mechanisms, the design of robust composite architectures to mitigate degradation, and the development of sustainable synthesis routes from biomass precursors.

Looking ahead, the convergence of AI-guided material discovery, advanced computational modeling, and green chemistry principles presents a transformative opportunity to accelerate

the development of N-CDs. With sustained and focused innovation, N-CDs are poised to bridge the critical gap between fundamental nanomaterial research and industrial-scale applications, ultimately enabling a new class of high-performance, sustainable, and commercially viable electrochemical energy storage technologies.

## Conflicts of interest

There are no conflicts to declare.

## Data availability

Data sharing is not applicable to this article as no datasets were generated or analysed during the current study.

## Acknowledgements

S. J. M. extends special thanks to the University of Sulaimani, College of Science, and the Chemistry Department for all of their cooperation.

## References

- 1 M. A. Hannan, M. M. Hoque, A. Mohamed and A. Ayob, *Renewable Sustainable Energy Rev.*, 2017, **69**, 771–789.
- 2 S. Ould Amrouche, D. Rekioua, T. Rekioua and S. Bacha, *Int. J. Hydrogen Energy*, 2016, **41**, 20914–20927.
- 3 I. Hadjipaschalidis, A. Poullikkas and V. Efthimiou, *Renewable Sustainable Energy Rev.*, 2009, **13**, 1513–1522.
- 4 D. Carolan, C. Rocks and D. B. Padmanaban, *et al.*, *Sustainable Energy Fuels*, 2017, **1**, 1611–1619.
- 5 Z. Bian, E. Gomez and M. Gruebele, *et al.*, *Chem. Sci.*, 2025, **16**, 4195–4212.
- 6 D. Cai, X. Zhong and L. Xu, *et al.*, *Chem. Sci.*, 2025, **16**, 4937–4970.
- 7 Y. Liu, S. Roy and S. Sarkar, *et al.*, *Carbon Energy*, 2021, **3**, 795–826.
- 8 Y. A. Kumar, J. K. Alagarasan and T. Ramachandran, *et al.*, *J. Energy Storage*, 2024, **86**, 111119.
- 9 Y. Anil Kumar, G. Koyyada and T. Ramachandran, *et al.*, *Nanomaterials*, 2023, **13**, 1049.
- 10 Y. A. Kumar, G. Koyyada and T. Ramachandran, *et al.*, *Dalton Trans.*, 2023, **52**, 8580–8600.
- 11 V. C. Hoang, K. Dave and V. G. Gomes, *Nano Energy*, 2019, **66**, 104093.
- 12 Z. Li, F. Liu and S. Chen, *et al.*, *Nano Energy*, 2021, **82**, 105698.
- 13 D. Lemian and F. Bode, *Energies*, 2022, **15**, 5683.
- 14 W. Hong, Y. Zhang and L. Yang, *et al.*, *Nano Energy*, 2019, **65**, 104038.
- 15 H. Jiang, L. Liu and K. Zhao, *et al.*, *Electrochim. Acta*, 2020, **337**, 135758.
- 16 S. N. Faisal, E. Haque and N. Noorbehesht, *et al.*, *RSC Adv.*, 2017, **7**, 17950–17958.



17 R. Guo, L. Li and B. Wang, *et al.*, *Energy Storage Mater.*, 2021, **37**, 8–39.

18 J.-S. Wei, T.-B. Song and P. Zhang, *et al.*, *Mater. Chem. Front.*, 2020, **4**, 729–749.

19 K. F. Kayani, M. K. Rahim and S. J. Mohammed, *et al.*, *J. Fluoresc.*, 2025, **35**, 2481–2494.

20 Z. R. Ismagilov, A. E. Shalagina and O. Y. Podyacheva, *et al.*, *Carbon*, 2009, **47**, 1922–1929.

21 R. Cheng, M. Jiang, K. Li, M. Guo, J. Zhang, J. Ren, P. Meng, R. Li and C. Fu, *Chem. Eng. J.*, 2021, **426**, 130603.

22 G. Zhang, J. Zhu, W. Zeng, S. Hou, F. Gong, F. Li, C. C. Li and H. Duan, *Nano Energy*, 2014, **10**, 269–277.

23 S. S. Siwal, H. Kaur, A. K. Saini and V. K. Thakur, *Adv. Energy Sustainability Res.*, 2022, **3**, 2200062.

24 J. Wu, Z. Pan and Y. Zhang, *et al.*, *J. Mater. Chem. A*, 2018, **6**, 12932–12944.

25 Q. Wu, L. Wang, Y. Yan, S. Li, S. Yu, J. Wang and L. Huang, *ACS Sustainable Chem. Eng.*, 2022, **10**, 9.

26 K. Yokwana, B. Ntsendwana, E. N. Nxumalo and S. D. Mhlanga, *J. Mater. Res.*, 2023, **38**, 3239–3263.

27 V. M. Naik, S. V. Bhosale and G. B. Kolekar, *Anal. Methods*, 2022, **14**, 877–891.

28 I. Y. Jeon, H. J. Noh and J. B. Baek, *Chem. – Asian J.*, 2020, **15**, 2282–2293.

29 A. Prakash, S. Yadav and U. Yadav, *et al.*, *Bull. Mater. Sci.*, 2023, **46**, 103.

30 K. F. Kayani, S. J. Mohammed and D. Ghafoor, *et al.*, *Mater. Adv.*, 2024, **5**, 4618–4633.

31 H. Liu, X. Zhong and Q. Pan, *et al.*, *Coord. Chem. Rev.*, 2024, **498**, 215468.

32 S. J. Mohammed, F. E. Hawaiz, S. B. Aziz and S. H. Al-Jaf, *Opt. Mater.*, 2024, **149**, 115014.

33 J. Tan, R. Zou and J. Zhang, *et al.*, *Nanoscale*, 2016, **8**, 4742–4747.

34 J. Manioudakis, F. Victoria and C. A. Thompson, *et al.*, *J. Mater. Chem. C*, 2019, **7**, 853–862.

35 R. Liu, D. Wu, X. Feng and K. Müllen, *J. Am. Chem. Soc.*, 2011, **133**, 15221–15223.

36 A. S. Rasal, T. M. Subrahmanyam and S. Kizhepat, *et al.*, *Coord. Chem. Rev.*, 2025, **533**, 216510.

37 S. J. Mohammed, M. K. Sidiq and H. H. Najmuldeen, *et al.*, *J. Environ. Chem. Eng.*, 2024, **12**, 114444.

38 M. S. Chaudhary, A. H. Anwer and S. Sultana, *et al.*, *Energy Fuels*, 2023, **37**, 18012–18042.

39 Y. Xie, D. Cheng, X. Liu and A. Han, *Sensors*, 2019, **19**, 3169.

40 Z. Lei, S. Xu, J. Wan and P. Wu, *Nanoscale*, 2016, **8**, 2219–2226.

41 Y. Deng, Y. Zhou, Q. Li and J. Qian, *Anal. Methods*, 2021, **13**, 3685–3692.

42 P. D. Modi, V. N. Mehta and V. S. Prajapati, *Inorg. Nano Met. Chem.*, 2022, **52**, 394–404.

43 T. Li, Y. Dong and Q. Yan, *et al.*, *Colloids Surf., A*, 2025, **705**, 135634.

44 G. He, M. Shu and Z. Yang, *et al.*, *Appl. Surf. Sci.*, 2017, **422**, 257–265.

45 M. Hasan, B. Baheerathan and S. Sutradhar, *et al.*, *Carbon Res.*, 2025, **4**, 49.

46 T. V. De Medeiros, J. Manioudakis and F. Noun, *et al.*, *J. Mater. Chem. C*, 2019, **7**, 7175–7195.

47 S. Bhatt, G. Vyas and P. Paul, *Anal. Methods*, 2022, **14**, 243–253.

48 Q. Xiao, Y. Liang and F. Zhu, *et al.*, *Anal. Bioanal. Chem.*, 2017, **409**, 4575–4583.

49 L. Fan, M. Zhu and X. Lee, *et al.*, *Part. Part. Syst. Charact.*, 2013, **30**, 764–769.

50 Y. Zhang, L. Li and S. Zhao, *et al.*, *Nano Res.*, 2024, **17**, 9174–9180.

51 S. Kumar, S. T. Aziz, O. Girshevitz and G. D. Nessim, *J. Phys. Chem. C*, 2018, **122**, 2343–2349.

52 S. Kumar, S. K. T. Aziz, O. Girshevitz and G. D. Nessim, *J. Phys. Chem. C*, 2018, **122**, 2343–2349.

53 D. Wei, Y. Liu and Y. Wang, *et al.*, *Nano Lett.*, 2009, **9**, 1752–1758.

54 N. Sharma and G. Kaur Bhullar, *Int. J. Innovative Sci. Res. Technol.*, 2023, **8**, 2931–2936.

55 F. Limosani, E. M. Bauer and D. Cecchetti, *et al.*, *Nanomaterials*, 2021, **11**, 2249.

56 K. Dimos, F. Arcudi and A. Kouloumpis, *et al.*, *Nanoscale*, 2017, **9**, 10256–10262.

57 Z. Jin, M. Liu and X. Huang, *et al.*, *Anal. Chem.*, 2022, **94**, 7609–7618.

58 S. Kang, Y. K. Jeong and J. H. Ryu, *et al.*, *Appl. Surf. Sci.*, 2020, **506**, 144998.

59 Á. Pérez Del Pino, A. Martínez Villarroyna and A. Chuquitarqui, *et al.*, *J. Mater. Chem. A*, 2018, **6**, 16074–16086.

60 R. L. Calabro, D.-S. Yang and D. Y. Kim, *ACS Appl. Nano Mater.*, 2019, **2**, 6948–6959.

61 R. Sinha, N. Roy and T. K. Mandal, *Langmuir*, 2023, **39**, 4518–4529.

62 R. L. Calabro, D. S. Yang and D. Y. Kim, *ACS Appl. Nano Mater.*, 2019, **2**, 6948–6959.

63 L. Shen, S. Zhou and F. Huang, *et al.*, *Nanotechnology*, 2021, **33**, 115602.

64 S. R. M. Santiago, T. N. Lin and C. H. Chang, *et al.*, *Phys. Chem. Chem. Phys.*, 2017, **19**, 22395–22400.

65 J. L. Speidell, D. P. Pulaski and R. S. Patel, *IBM J. Res. Dev.*, 1997, **41**, 143–148.

66 G.-S. Kang, S. Lee and J.-S. Yeo, *Chem. Eng. J.*, 2019, **372**, 624–630.

67 Y. Yang, W. Shi and R. Zhang, *et al.*, *Electrochim. Acta*, 2016, **204**, 100–107.

68 M. Jing, T. Wu and Y. Zhou, *et al.*, *Front. Chem.*, 2020, **8**, 1–10.

69 D. B. Shinde, V. M. Vishal, S. Kurungot and V. K. Pillai, *Bull. Mater. Sci.*, 2015, **38**, 435–442.

70 Y. Fu, G. Gao and J. Zhi, *J. Mater. Chem. B*, 2019, **7**, 1494–1502.

71 F. Lou, M. E. M. Buan and N. Muthuswamy, *et al.*, *J. Mater. Chem. A*, 2016, **4**, 1233–1243.

72 K. Chu, J. R. Adsetts and S. He, *et al.*, *Chem. – Eur. J.*, 2020, **26**, 15892–15900.



73 Q. Zhou, G. Yuan and M. Lin, *et al.*, *J. Mater. Sci.*, 2021, **56**, 12909–12919.

74 F. Wang, S. Wang, Z. Sun and H. Zhu, *Fullerenes, Nanotubes and Carbon Nanostruct.*, 2015, **23**, 769–776.

75 Y. Zhang, M. Park and H. Y. Kim, *et al.*, *Sci. Rep.*, 2017, **7**, 45086.

76 J. Xu, K. Cui and T. Gong, *et al.*, *Colloids Surf., A*, 2022, **644**, 128828.

77 Y. Zhang, M. Park and H. Y. Kim, *et al.*, *Sci. Rep.*, 2017, **7**, 45086.

78 Z. Ma, H. Ming and H. Huang, *New J. Chem.*, 2012, **36**, 861–864.

79 T. N. J. I. Edison, R. Atchudan and M. G. Sethuraman, *et al.*, *Spectrochim. Acta, Part A*, 2016, **165**, 128–137.

80 T. Y. Shen, P. Y. Jia, D. S. Chen and L. N. Wang, *Spectrochim. Acta, Part A*, 2021, **248**, 119282.

81 R. Atchudan, T. N. J. I. Edison and D. Chakradhar, *et al.*, *Sens. Actuators, B*, 2017, **246**, 497–509.

82 L. Zhao, Y. Wang and X. Zhao, *et al.*, *Polymers*, 2019, **11**, 1731.

83 A. Ghanem, R. A. B. Al-marjeh and Y. Atassi, *Helijon*, 2020, **6**, e03750.

84 T.-Y. Shen, P.-Y. Jia, D.-S. Chen and L.-N. Wang, *J. Fluoresc.*, 2021, **31**, 1145–1155.

85 Y. N. Monday, J. Abdullah and N. A. Yusof, *et al.*, *Appl. Sci.*, 2021, **11**, 1630.

86 C. Qi, H. Wang and A. Yang, *et al.*, *ACS Omega*, 2021, **6**, 32904–32916.

87 S. Aydin, O. Ustun and A. Ghosigharehaghaji, *et al.*, *Coatings*, 2022, **12**, 1311.

88 P. Liu, G. Ai, Y. Wang and J. Ai, *Molecules*, 2023, **28**, 6607.

89 G. Magdy, F. Belal and H. Elmansi, *RSC Adv.*, 2023, **13**, 4156–4167.

90 Y. Hu, J. Yang, J. Tian and J.-S. Yu, *J. Mater. Chem. B*, 2015, **3**, 5608–5614.

91 W. Tan, R. Fu and H. Ji, *et al.*, *Int. J. Biol. Macromol.*, 2018, **112**, 561–566.

92 Y. Zhao, C. Hu and Y. Hu, *et al.*, *Angew. Chem., Int. Ed.*, 2012, **51**, 11371–11375.

93 S. B. Aziz, R. T. Abdulwahid and S. Al-Zangana, *et al.*, *J. Energy Storage*, 2025, **123**, 116765.

94 S. Majeed, J. Zhao and L. Zhang, *et al.*, *Nanotechnol. Rev.*, 2013, **2**, 615–635.

95 N. Gavrilov, I. A. Pašti and M. Vujković, *et al.*, *Carbon*, 2012, **50**, 3915–3927.

96 J. Zhao, Y. Liu and X. Quan, *et al.*, *Appl. Surf. Sci.*, 2017, **396**, 986–993.

97 A. Marpongahtun, Y. Andriayani and Y. Muis, *et al.*, *Int. J. Technol.*, 2023, **14**, 219–231.

98 S. A. Shaik, S. Sengupta and R. S. Varma, *et al.*, *ACS Sustainable Chem. Eng.*, 2021, **9**, 3–49.

99 H. Wang, L. Ai and Z. Song, *et al.*, *Chem. – Eur. J.*, 2023, **29**, e202302383.

100 K. Yokwana, B. Ntsendwana, E. N. Nxumalo and S. D. Mhlanga, *J. Mater. Res.*, 2023, **38**, 3239–3263.

101 R. Palmbahs, P. Lesnicenoks and A. Knoks, *et al.*, *ChemEngineering*, 2024, **8**, 80.

102 X. Mao, G. C. Rutledge and T. A. Hatton, *Nano Today*, 2014, **9**, 405–432.

103 Z. Luo, S. Lim and Z. Tian, *et al.*, *J. Mater. Chem.*, 2011, **21**, 8038–8044.

104 M. Li, C. Liu, H. Cao, J. Pan, H. Zhao and Y. Zhang, *Mater. Chem. Phys.*, 2015, **152**, 77–84.

105 G. Gao, M. Pan and C. Vecitis, *J. Mater. Chem. A*, 2015, **3**, 4843–4853.

106 D. J. Nelson, N. Vasimalai, S. A. John and M. G. Sethuraman, *J. Fluoresc.*, 2025, **35**, 963–974.

107 R. Kamaraj, N. Nesakumar and S. Vasudevan, *Chem. Commun.*, 2020, **56**, 10034–10040.

108 X. Wang, G. Sun and P. Routh, *et al.*, *Chem. Soc. Rev.*, 2014, **43**, 7067–7098.

109 Y. Xu, M. Wu and Y. Liu, *et al.*, *Chem. – Eur. J.*, 2013, **19**, 2276–2283.

110 H. Jiang, L. Liu and K. Zhao, *et al.*, *Electrochim. Acta*, 2020, **337**, 135758.

111 D. Carolan, C. Rocks and D. B. Padmanaban, *et al.*, *Sustainable Energy Fuels*, 2017, **1**, 1611–1619.

112 S. S. Siwal, H. Kaur, A. K. Saini and V. K. Thakur, *Adv. Energy Sustainability Res.*, 2022, **3**, 2200062.

113 X. You, M. Misra, S. Gregori and A. K. Mohanty, *ACS Sustainable Chem. Eng.*, 2018, **6**, 318–324.

114 J. D. Wiggins-Camacho and K. J. Stevenson, *J. Phys. Chem. C*, 2009, **113**, 19082–19090.

115 K. Murugan, V. K. Jothi, R. Arulmozhi and A. Natarajan, *ACS Omega*, 2021, **6**, 35848–35860.

116 N. Qutub, B. Pirzada, K. Umar and S. Sabir, *J. Environ. Chem. Eng.*, 2015, **4**, 661–670.

117 B. Şenel, N. Demir, G. Büyükköroğlu and M. Yıldız, *Saudi Pharm. J.*, 2019, **27**, 846–858.

118 M. A. Barote, A. A. Yadav and E. U. Masumdar, *Phys. B*, 2011, **406**, 2567–2572.

119 S. S. A. S. Arumugam and S. Jose, *et al.*, *J. Mater. Sci.*, 2024, **59**, 21846–21867.

120 Y. Liu, L. Jiang and B. Li, *et al.*, *J. Mater. Chem. B*, 2019, **7**, 3364–3371.

121 A. Prakash, S. Yadav and U. Yadav, *et al.*, *Bull. Mater. Sci.*, 2023, **46**, 103.

122 X. Kou, X. Xin, Y. Zhang and L.-Y. Meng, *Carbon Lett.*, 2021, **31**, 885–896.

123 Z. Zhong, S. Mahmoodi, D. Li and S. Zhong, *Metals*, 2022, **12**, 2166.

124 M. Sheikh, R. Chandok and K. Abida, *Discover Mater.*, 2024, **4**, 79.

125 J. D. Bagley, K. Kumar and K. A. See, *RSC Adv.*, 2020, **10**, 39562–39571.

126 J. Guo, S. C. Abbas and H. Huang, *et al.*, *J. Colloid Interface Sci.*, 2023, **641**, 155–165.

127 M. Sivakumar, S. Mani and S.-M. Chen, *et al.*, *Int. J. Electrochem. Sci.*, 2017, **12**, 5092–5103.

128 B. Matsoso, K. Ranganathan and B. Mutuma, *et al.*, *RSC Adv.*, 2016, **6**, 108928–108937.



129 M. Matsuoka, *World J. Nano Sci. Eng.*, 2012, **2**, 92–102.

130 H. Bai, Y. Yang and Y. Huang, *et al.*, *Appl. Catal. B*, 2025, **365**, 125001.

131 K. Chang, Q. Zhu and L. Qi, *et al.*, *Materials*, 2022, **15**, 466.

132 Y. Li, G. Shi and C. Xu, *et al.*, *J. Power Sources*, 2024, **619**, 235200.

133 L. Cui, X. Ren and M. Sun, *et al.*, *Nanomaterials*, 2021, **11**, 3419.

134 V. T. Nguyen, K. Cho and Y. Choi, *et al.*, *Biochar*, 2024, **6**, 34.

135 M. D. Nešić, I. A. Popović and J. Žakula, *et al.*, *Pharmaceutics*, 2024, **16**, 671.

136 S. H. Kim, J. Y. Park and S. Y. Choi, *et al.*, *Nano Energy*, 2025, **142**, 111170.

137 D.-H. Liu, C. Xu and F. Xu, *et al.*, *Carbon Neutralization*, 2025, **4**, e70014.

138 S. Cho, H. Kim, D. Song, J. H. Kim, T. Hyeon and J. Park, *Sci. Rep.*, 2024, **14**, 22456.

139 C. Ma, X. Xu and M. Xu, *et al.*, *J. Mater. Chem. A*, 2025, **13**, D4TA08732A.

140 H. Li, Y. Xie, Y. Liu, Y. Xiao, H. Hu, Y. Liang and M. Zheng, *RSC Adv.*, 2021, **11**, 10785–10793.

141 M. Chen, J. Ma and Y. Feng, *et al.*, *Coord. Chem. Rev.*, 2025, **535**, 216612.

142 Q. Hou, B. Xing and H. Guo, *et al.*, *New J. Chem.*, 2022, **46**, 17102–17113.

143 M. Wang, X. Li and L. Liu, *et al.*, *Energy Storage Mater.*, 2024, **65**, 103110.

144 M. C. Franklin, S. Manickam and L. Sunil, *et al.*, *ACS Appl. Mater. Interfaces*, 2024, **16**, 50587–50601.

145 J. Dai, G. Li, Y. Hu and L. Han, *J. Energy Storage*, 2024, **83**, 110640.

146 A. I. Alakhras, H. Idriss and S. Dueby, *et al.*, *Diamond Relat. Mater.*, 2025, **159**, 112787.

147 J. Yu, N. Fu and J. Zhao, *et al.*, *ACS Omega*, 2019, **4**, 15904–15911.

148 D. Liu, S. Kim and W. M. Choi, *Materials*, 2024, **17**, 884.

149 H. M. Jeong, S. Y. Lee and W. H. Shin, *et al.*, *RSC Adv.*, 2012, **2**, 4311–4317.

150 B. Huang, B. Chu, T. Huang and A. Yu, *Molecules*, 2021, **26**, 1536.

151 Z. Nie, Y. Huang and B. Ma, *et al.*, *Sci. Rep.*, 2019, **9**, 15032.

152 X. Li and X. Sun, *Front. Energy Res.*, 2014, **2**, 49.

153 C. Gao, Q. Wang and S. Luo, *et al.*, *J. Power Sources*, 2019, **415**, 165–171.

154 B. Bajorowicz, M. Wilamowska-Zawłocka and W. Lisowski, *et al.*, *Appl. Surf. Sci.*, 2024, **655**, 159702.

155 J. H. Park, J.-H. Shin and J.-M. Ju, *et al.*, *Nano Convergence*, 2022, **9**, 17.

156 X. Kou, X. Xin, Y. Zhang and L.-Y. Meng, *Carbon Lett.*, 2021, **31**, 695–706.

157 Q. Yang, Z. Xie and D. He, *et al.*, *J. Ind. Eng. Chem.*, 2025, **148**, 614–621.

158 R. Genc, M. O. Alas and E. Harputlu, *et al.*, *Sci. Rep.*, 2017, **7**, 11222.

159 D. Huang, Y. Chen and M. Cheng, *et al.*, *Small*, 2021, **17**, 2002998.

160 Z. Jiang, L. Guan and X. Xu, *et al.*, *ACS Appl. Electron. Mater.*, 2022, **4**, 1152.

161 L. Cui, Y. An and H. Xu, *et al.*, *New J. Chem.*, 2021, **45**, 21692–21700.

162 A. I. Alakhras, H. Idriss and S. Dueby, *et al.*, *Diamond Relat. Mater.*, 2025, **159**, 112787.

163 S. Wang, J. Deng and M. Li, *et al.*, *Chem. Eng. J.*, 2025, **511**, 162275.

164 Y. Zhang, L. Yue and H. Ding, *et al.*, *Nano Energy*, 2024, **127**, 109696.

165 M. Wang, Z. Fang and K. Zhang, *et al.*, *Nanoscale*, 2016, **8**, 11398–11402.

166 P. Zhang, D. Bin and J.-S. Wei, *et al.*, *ACS Appl. Mater. Interfaces*, 2019, **11**, 14085–14094.

167 Z. Qin, P. Xia and X. Liu, *et al.*, *J. Energy Storage*, 2025, **121**, 116628.

168 D. Khalafallah, D. E. El Refaay and X. Gu, *et al.*, *Energy Storage Mater.*, 2025, **78**, 104284.

169 Y.-C. Hsiao, J.-L. Hung and S. Kubendhiran, *et al.*, *J. Energy Storage*, 2022, **56**, 105902.

170 K. Poonam, K. Sharma, A. Arora and S. K. Tripathi, *J. Energy Storage*, 2019, **21**, 801–825.

171 X. Wang, L. Tian and X. Long, *et al.*, *Sci. China Mater.*, 2021, **64**, 1632–1641.

172 M. A. Sheikh, R. S. Chandok and K. Abida, *Discover Nano*, 2023, **18**, 132.

173 S. Wang, J. Deng and M. Li, *et al.*, *Chem. Eng. J.*, 2025, **511**, 162275.

174 Z. Li, F. Bu and J. Wei, *et al.*, *Nanoscale*, 2018, **10**, 22871–22883.

175 S. B. Aziz, P. O. Hama and P. A. Mohammed, *et al.*, *J. Energy Storage*, 2024, **103**, 114264.

176 A. A. M. Farag, I. S. Yahia and M. Fadel, *Int. J. Hydrogen Energy*, 2009, **34**, 4906–4913.

177 S. B. Aziz, P. O. Hama and D. M. Aziz, *et al.*, *J. Energy Storage*, 2025, **114**, 115841.

178 C. Deng, J. He and G. Wang, *et al.*, *Appl. Surf. Sci.*, 2023, **616**, 156526.

179 M. I. A. Abdel Maksoud, R. A. Fahim and A. E. Shalan, *et al.*, *Environ. Chem. Lett.*, 2021, **19**, 375–439.

180 G. Yuan, X. Zhao and Y. Liang, *et al.*, *J. Colloid Interface Sci.*, 2019, **536**, 628–637.

181 K. A. Othman, L. I. A. Ali and A. F. Qader, *et al.*, *J. Fluoresc.*, 2024, **34**, 3736.

182 R. Cheng, Y. Xiang and R. Guo, *et al.*, *Small*, 2021, **17**, 2102091.

183 N. C. Joshi, *Ionics*, 2025, **31**, 6264.

184 L. Ruiyi, J. Yuanyuan and Z. Xiaoyan, *et al.*, *Electrochim. Acta*, 2015, **178**, 303–311.

185 S. Yang, X. Ye and N. Shen, *et al.*, *Chem. – Eur. J.*, 2025, **31**, e202402794.

186 Y. Yang, X. Ji and M. Jing, *et al.*, *J. Mater. Chem. A*, 2015, **3**, 5648–5655.

187 X. Li, S. Yu, X. Zhao and J. Liu, *Energy Storage Mater.*, 2025, **79**, 104303.



188 C. Tang, H. Tao, X. Liu and X. Yang, *Energy Fuels*, 2022, **36**, 1043–1051.

189 L. Mezzomo, C. Ferrara and G. Brugnetti, *et al.*, *Adv. Energy Mater.*, 2020, **10**, 2002815.

190 Md. M. Chand, S. Islam and M. T. Ahmed, *et al.*, *AIP Adv.*, 2023, **13**, 125225.

191 X.-Q. Zhang, S. Tang and Y.-Z. Fu, *J. Electrochem.*, 2023, **29**, 2217005.

192 B. Jiang, Y. Liang and X. Yu, *et al.*, *J. Alloys Compd.*, 2020, **838**, 155508.

193 K. Dahmani, O. Kharbouch and M. Galai, *ACS*, 2024, **149**, 165.

194 H. Li, Y. Xie and Y. Liu, *et al.*, *RSC Adv.*, 2021, **11**, 10785–10793.

195 S. Wang, H. Wang and R. Zhang, *et al.*, *J. Alloys Compd.*, 2018, **746**, 567–575.

196 H. Wu, Q. Yu and C.-Y. Lao, *et al.*, *Energy Storage Mater.*, 2019, **18**, 43–50.

197 J.-W. Ni, X.-R. Zhang and T.-B. Song, *et al.*, *Chem. Eng. J.*, 2024, **500**, 157379.

198 Y. Xiang, L. Xu, L. Yang, Y. Ye, Z. Ge, J. Wu, W. Deng, G. Zou, H. Hou and X. Ji, *Nano-Micro Lett.*, 2022, **14**, 136.

199 D. Kong, Y. Wang and S. Huang, *et al.*, *J. Mater. Chem. A*, 2019, **7**, 12751–12762.

200 D. Zhao, Y. Wang, G. Chang, C. Chen, Q. Kong, Z. Li and H. Zhao, *ACS Appl. Nano Mater.*, 2022, **5**, 14912–14920.

201 S. Yadav and S. Daniel, *Energy Storage*, 2024, **6**, e500.

202 M. Shaker, T. Shahalizade and A. Mumtaz, *et al.*, *FlatChem*, 2023, **40**, 100516.

203 H. Ying, S. Zhang and Z. Meng, *et al.*, *J. Mater. Chem. A*, 2017, **5**, 8334–8342.

204 J.-I. Lee, S. Cho and S. H. Kim, *et al.*, *Energy Storage Mater.*, 2025, **75**, 104023.

205 Z. Li, Q. Gan and Y. Zhang, *et al.*, *Nano Res.*, 2022, **15**, 217–224.

206 W. Xu, F. Zeng, Q. Han and Z. Peng, *Coord. Chem. Rev.*, 2024, **498**, 215469.

207 M. I. Hossain, F. K. Tareq and S. Rudra, *Energy Storage Mater.*, 2025, **75**, 104025.

208 G. Li, Q. Chen and J. Feng, *et al.*, *Energy Storage Mater.*, 2025, **78**, 104282.

209 Y. Xue, H. Zhou and Z. Ji, *et al.*, *Appl. Surf. Sci.*, 2023, **633**, 157580.

210 T.-W. Chen, S.-M. Chen and G. Anushya, *et al.*, *Int. J. Electrochem. Sci.*, 2024, **19**, 100548.

211 G. Gollavelli, G. Gedda, R. Mohan and Y.-C. Ling, *Molecules*, 2022, **27**, 7851.

212 S. Li, Y. Wang and Y. Ding, *et al.*, *Chem. Eng. J.*, 2022, **430**, 132969.

213 N. Selvaraju, S. Sasi, Y. Sivalingam and G. Venugopal, *Diamond Relat. Mater.*, 2024, **148**, 111362.

214 H. Zhang, B. Wang and X. Yu, *et al.*, *Angew. Chem.*, 2020, **132**, 19558–19570.

215 G. Long, Y. Liu and M. Chen, *et al.*, *J. Power Sources*, 2023, **573**, 233150.

216 P. Zhang, J.-S. Wei, X.-B. Chen and H.-M. Xiong, *J. Colloid Interface Sci.*, 2019, **537**, 716–724.

217 X. Lin, K. Gao and Y. Han, *et al.*, *J. Nanopart. Res.*, 2022, **24**, 52.

218 F. Sher, I. Ziani and M. Smith, *et al.*, *Coord. Chem. Rev.*, 2024, **500**, 215499.

219 L. Peng, L. Hu and X. Fang, *Adv. Funct. Mater.*, 2014, **24**, 2591–2610.

220 A. T. Nguyet Nguyen and J. H. Shim, *RSC Adv.*, 2021, **11**, 12520–12530.

221 Z. Ji, K. Liu, W. Dai, D. Ma, H. Zhang, X. Shen, G. Zhu and S. Wu, *Nanoscale*, 2021, **13**, 1689–1695.

222 C. Hu, C. Yu and M. Li, *et al.*, *Chem. Commun.*, 2015, **51**, 3419–3422.

223 R. Genc, M. O. Alas, E. Harputlu, S. Repp, N. Kremer, M. Castellano, S. G. Colak, K. Ocakoglu and E. Erdem, *Sci. Rep.*, 2017, **7**, 11222.

224 Z. Ji, N. Li and Y. Zhang, *et al.*, *J. Colloid Interface Sci.*, 2019, **542**, 392–399.

225 R. Yuksel, E. Alpugan and H. E. Unalan, *Org. Electron.*, 2018, **52**, 272–280.

226 M. M. Rahman, M. R. Shawon and M. H. Rahman, *et al.*, *J. Energy Storage*, 2023, **67**, 107615.

227 G.-L. Xu, Y. Li and T. Ma, *et al.*, *Nano Energy*, 2015, **18**, 253–264.

228 B. Ballarin, E. Boanini, L. Montalto, P. Mengucci, D. Nanni, C. Parise, I. Ragazzini, D. Rinaldi, N. Sangiorgi, A. Sanson and M. C. Cassani, *Electrochim. Acta*, 2019, **318**, 134707.

229 A. T. Lawal, *Carbon Trends*, 2025, **19**, 100470.

230 S. B. Aziz, O. G. Abdullah, D. M. Aziz, M. B. Ahmed and R. T. Abdulwahid, *ACS Appl. Electron. Mater.*, 2024, **6**, 11.

231 H. Joo, D. Jung and S.-H. Sunwoo, *et al.*, *Small*, 2020, **16**, 1906270.

232 M. Zulfajri, S. Sudewi and S. Ismulyati, *et al.*, *Coatings*, 2021, **11**, 1100.

233 N. A. Shamsuri, S. N. A. Halim and S. B. Aziz, *et al.*, *J. Energy Storage*, 2024, **102**, 113909.

234 F. Xie, M. Zhou and G. Wang, *et al.*, *Int. J. Energy Res.*, 2019, **43**, 7529–7540.

235 L. Lu and Y. Xie, *J. Mater. Sci.*, 2019, **54**, 4842–4858.

236 L. Feng, M. Wang and Y. Chang, *et al.*, *ACS Appl. Energy Mater.*, 2023, **6**, 7147–7155.

237 A. Singh, S. R. Kafle, M. Sharma and B. S. Kim, *Catalysts*, 2023, **13**, 1446.

238 N. B. Sonawane, K. V. Gurav and R. R. Ahire, *et al.*, *Sens. Actuators, A*, 2014, **216**, 78–83.

239 M. Yasa, A. Deniz, M. Forough, E. Yildirim, O. P. Cetinkol, Y. Arslan Uдум and L. Toppare, *J. Polym. Sci.*, 2020, **58**, 647.

240 T. Sen, S. Mishra and N. G. Shimpi, *RSC Adv.*, 2016, **6**, 42196–42222.

241 N. Punnakkal, S. Naneena and S. L. Cp, *et al.*, *J. Energy Storage*, 2024, **100**, 113527.

242 F. Xie, M. Zhou and G. Wang, *et al.*, *Int. J. Energy Res.*, 2019, **43**, 7529–7540.

243 H. M. El Sharkawy, A. S. Dhmees and A. R. Tamman, *et al.*, *J. Energy Storage*, 2020, **27**, 101078.

244 Y. Sahu, A. Hashmi and R. Patel, *et al.*, *Nanomaterials*, 2022, **12**, 3434.



245 X. Rui, H. Tan and Q. Yan, *Nanoscale*, 2014, **6**, 9889–9924.

246 X. Y. Yu and X. W. (David) Lou, *Adv. Energy Mater.*, 2018, **8**, 1701592.

247 V. Sharavath, S. Sarkar and S. Ghosh, *J. Electroanal. Chem.*, 2018, **829**, 208–216.

248 W. Xia, A. Mahmood, R. Zou and Q. Xu, *Energy Environ. Sci.*, 2015, **8**, 1837–1866.

249 S. S. Siwal, H. Kaur, A. K. Saini and V. K. Thakur, *Adv. Energy Sustainability Res.*, 2022, **3**, 2200062.

250 S. B. Aziz, R. T. Abdulwahid and D. M. Aziz, *et al.*, *Mater. Chem. Phys.*, 2024, **322**, 129607.

251 B. Zhang, Y. Tian, F. Chi and S. Liu, *Electrochim. Acta*, 2021, **390**, 138821.

252 R. Sinha, N. Roy and T. K. Mandal, *Langmuir*, 2023, **39**, 4518–4529.

253 T. Li, Y. Dong, J. Zhang and Y. Su, *Int. J. Hydrogen Energy*, 2024, **87**, 76–88.

254 Z. Ji, N. Li and M. Xie, *et al.*, *Electrochim. Acta*, 2020, **334**, 135632.

255 L. Cui, H. Xu, L. Zhang and X. Jin, *Polymers*, 2024, **16**, 2959.

256 J. Yu, H. Song and X. Li, *et al.*, *Adv. Funct. Mater.*, 2021, **31**, 2107196.

257 B. Lu, G.-T. Xiang and J.-L. Xu, *et al.*, *J. Energy Storage*, 2024, **91**, 112039.

258 S. Wang, J. Deng, M. Li, J. Lin, L. Luo, Z. Yuan, W. Zhang, C. He, G. Du and W. Zhao, *Chem. Eng. J.*, 2025, **487**, 162275.

259 Z. Wang, H. Che and W. Lu, *et al.*, *Adv. Sci.*, 2023, **10**, 2301355.

260 X. Guan, X. Xu and Y. Wu, *et al.*, *Nanomaterials*, 2023, **13**, 2989.

261 N. Kaushal, A. L. Sharma and A. Saha, *Mater. Adv.*, 2022, **3**, 355–361.

262 M. Moniruzzaman and J. Kim, *Sens. Actuators, B*, 2019, **295**, 12–21.

263 N. Zahir, P. Magri and W. Luo, *Energy Environ. Mater.*, 2022, **5**, 201–214.

264 Z. Wei, W. Lu and X. Wang, *et al.*, *J. Mater. Chem. C*, 2022, **10**, 1932–1967.

265 Z. Li, Y. Li and L. Wang, *et al.*, *Electrochim. Acta*, 2017, **235**, 561–569.

266 Y. Zhai, B. Zhang and R. Shi, *et al.*, *Adv. Energy Mater.*, 2022, **12**, 2103426.

267 S. Varadharajan, K. S. Vasanthan and V. Mathur, *et al.*, *Discover Nano*, 2024, **19**, 205.

268 S. Yang, X. Ye and N. Shen, *et al.*, *Chem. – Eur. J.*, 2025, **31**, e202402794.

269 L. Chen, C.-F. Wang, C. Liu and S. Chen, *Small*, 2023, **19**, 2206671.

270 D. Kumar, M. Rahamathulla and M. S. Ilango, *et al.*, *Energy Storage*, 2024, **6**, e498.

271 S. Ravi and S. Vadukumpally, *J. Environ. Chem. Eng.*, 2016, **4**, 835–856.

